

The oleic acid-ozone heterogeneous reaction system: products, kinetics, secondary chemistry, and atmospheric implications of a model system – a review

J. Zahardis and G. A. Petrucci

Department of Chemistry, University of Vermont, Burlington, VT 05405-0125, USA

Received: 18 October 2006 – Accepted: 26 October 2006 – Published: 9 November 2006

Correspondence to: G. A. Petrucci (giuseppe.petrucci@uvm.edu)

11093

Abstract

The heterogeneous processing of organic aerosols by trace oxidants has many implications to atmospheric chemistry and climate regulation. This review covers a model heterogeneous reaction system (HRS): the oleic acid-ozone HRS and other reaction systems featuring fatty acids, and their derivatives. The analysis of the primary products of ozonolysis (azelaic acid, nonanoic acid, 9-oxononanoic acid, nonanal) is described. Anomalies in the relative product yields are noted and explained by the observation of secondary chemical reactions. The secondary reaction products arising from reactive Criegee intermediates are mainly peroxidic, notably secondary ozonides and α -acyloxyalkyl hydroperoxide polymers. These highly oxygenated products are of low volatility and hydrophilic which may enhance the ability of particles to act as cloud condensation nuclei. The kinetic description of this HRS is critically reviewed. Most kinetic studies suggest this oxidative processing is either a near surface reaction that is limited by the diffusion of ozone or a surface based reaction. Internally mixed particles and coatings represent the next stage in the progression towards more realistic proxies of tropospheric organic aerosols and a description of the products and the kinetics resulting from the ozonolysis of these proxies, which are based on fatty acids or their derivatives, is presented. Finally, a series of atmospheric implications of oxidative processing of particulate containing fatty acids is presented. These implications include the extended lifetime of unsaturated species in the troposphere facilitated by the presence of solids, semisolids or viscous phases, and an enhanced rate of ozone uptake by particulate unsaturates compared to corresponding gas phase organics. Ozonolysis of oleic acid enhances its CCN activity, which implies that oxidatively processed particulate may contribute to indirect forcing of radiation. Other effects, including the potential role of aldehydic products of ozonolysis in increasing the oxidative capacity of the troposphere, are also discussed.

11094

1 Introduction

As of late the atmospheric chemistry and physics research community has been giving increasing attention to the role of organic aerosols (OA) in the troposphere. A recent workshop organized by the International Geosphere Biosphere Programme (IGBP) – International Global Atmospheric Chemistry Project (IGAC), Integrated Land Ecosystem Process Study (iLEAPS), and Surface Ocean-Lower Atmosphere Study (SOLAS) was held on atmospherically related phenomena and has been summarized (Fuzzi et al., 2006). In regards to OA four broad areas of concern were addressed: 1) sources; 2) formation and transformation; 3) physical and chemical state, and 4) atmospheric modeling.

We present a summary of experimental results and implications in one of the key OA reaction systems: the oleic acid-ozone heterogeneous reaction system (OL-O₃ HRS; OL is 9-octadecenoic acid) and address points 2) and 3) above, with implications to 4). The results of these studies suggest that oxidatively processed OA may be good cloud condensation nuclei (CCN) suggesting OA may play an important role in climate regulation by indirect aerosol effects.

1.1 Sources of organic acids and fatty acids

Organic acids are ubiquitous in the troposphere and fatty acids (FA) make up a significant contribution to this fraction (Cheng et al., 2004; Duce et al., 1983; Hahn, 1980; Limbeck and Puxbaum, 1999). These FA have both anthropogenic and biogenic sources. Anthropogenic sources of FA include automobile exhaust (Cheng et al., 2004; Huang et al., 2005), other types of fossil fuel combustion (Simoneit, 1985, 1986), and cooking emissions (Guo et al., 2003; He et al., 2004; Huang et al., 2005; Rogge et al., 1991; Schauer et al., 1999). Biomass burning is noted as being a viable source of organic emissions (Decesari et al., 2006; Hoffer et al., 2005; Mayol-Bracero et al., 2002; Reid et al., 2005), including organic acids, and this source along with leaf-abrasion (Rogge et al., 1993) may be significant sources of FA particulate and have

11095

been associated with the dense coatings of these lipids on atmospheric aerosols in clean regions in western USA (Seidl, 2000). Another recently noted potential source of OA is fugitive dust emission (Ashbaugh et al., 2003), including emissions from cattle feedlots (Rogge et al., 2006), with FA being a significant fraction of these emissions. In rural and remote continental locations, direct forest emissions, especially from vascular plants, are also a significant biogenic source of FA (Cheng et al., 2004; Pio et al., 2001; Simoneit et al., 1988; Simoneit et al., 1991; Simoneit and Mazurek, 1982) and other organic acids. Biological degradation of plankton and other marine microorganisms is a significant biogenic source of FA in the marine environment (Barger and Garrett, 1970; Bezdek and Carlucci, 1974; Marty et al., 1979; Mayol-Bracero et al., 2001), with particles rich in organics formed from primary emissions via a bubble bursting mechanism in the marine boundary layer (Barger and Garrett, 1970; Bezdek and Carlucci, 1974; Blanchard, 1964; O'Dowd et al., 2004).

1.2 Some implications of oxidative processing of fatty acids

The role of OA, including organic acids, in acting as CCN has been investigated (Broekhuizen et al., 2004; Facchini et al., 1999; Herrmann et al., 2005; Kanakidou et al., 2005; Kumar et al., 2003; Sun and Ariya, 2006; Yu, 2000). It has been found that lower MW organic acids in the submicron regime, such as oxalic, malonic and glutaric acids, act in accord with Köhler's theory and are CCN active. However, poorly soluble, HMW FA do not activate upon supersaturation (Kumar et al., 2003). Unsaturated FA that are susceptible to oxidative processing have increased CCN capabilities (Broekhuizen et al., 2004). In this report we will focus on the oxidative processing of unsaturated FA with special attention to the OL-O₃ HRS.

Recent experiments suggest that ozonolysis can change significantly the physical characteristics of OL. For example, quartz crystal microbalance studies (Asad et al., 2004) have shown the rapid increase of the water-sorbing capacity of OL thin films upon exposure to ozone. It was observed that the fully oxidized film can take up about four times the amount of water as the unprocessed film, and may contain oxygenated

11096

polymers.

Pure OL and mixed OL/methanol particles behave differently in terms of CCN activity. In studies that employed tandem differential mobility analyzers, OL acid was not an effective CCN for particles with a diameter of less than 300 nm at a supersaturation less than or equal to one-percent. However, mixed OL-methanol particles had a critical activation diameter of 188 nm at 0.6% supersaturation (Broekhuizen et al., 2004). It was also found that while all submicron particles decreased in size upon moderate ozone exposure only the mixed particles became active under these conditions. For the pure OL particles, a much higher ozone exposure was necessary for activation.

Other particulate properties may be affected by exposure to ozone. OL-coated polystyrene latex spheres showed an increase of density upon exposure to ozone (Katrib et al., 2005b). Interestingly, the density and O:C ratio increased even after all the OL had reacted, implying a rich secondary chemistry. The increase in O:C ratio is significant in that this property correlates with the formation of water-soluble organics that have been noted as being good candidates for CCN (Facchini, 2001; Facchini et al., 1999; Kumar et al., 2003). Less is known about the role that organic acids could play in homogeneous ice formation, but studies are underway to investigate their purported role (Kärcher and Koop, 2005).

– The key implication of observations to date is that ozonolysis causes an increase in the O:C ratio which is associated with an increase in CCN ability

1.3 Scope of this review

It is clear that exposure to ozone has a strong effect on the chemical composition and physical properties of OL particles and has strong atmospheric implications. Therefore, there is a need to develop a better description of the oxidative processing of OA in the atmosphere. This includes a more detailed chemical and microphysical description of ozonolysis that includes reactive uptake, product description, and accounts for secondary reactions. Most importantly, correlation must be drawn between the roles of oxidative processing and the impact that OA has on atmospheric processes, such as

11097

indirect aerosol effects, where great uncertainty remains.

In light of this, we present what has been learned about the OL-O₃ HRS as of late. After a brief review of experimental methodologies, focus will be on describing the types and yields of products of the OL-O₃ HRS with emphasis on secondary chemistry. This is followed by a brief description of the resistor model of reactive uptake and a summary of the measurements of the reactive uptake of ozone by OL and related systems. Also discussed will be the kinetics of internally mixed particles and coatings, and the effects of phase equilibria, morphology, and other factors on reactive uptake.

The discussion will focus on the broad tropospheric implications of oxidative processing of OA, from the perspective of what we have learned from this model system. Special attention will be given to the role of oxidized OA in acting as CCN, and its effect on the radiation budget.

2 Methodology

Two main methodologies have been employed to study the OL-O₃ HRS: coated flow tubes (CFT) and aerosol flow tubes (AFT) (Rudich, 2003). Both methodologies typically rely on mass spectral detection of chemical products. They differ in the way the organic-phase is presented to the trace oxidizing gas (cf. coating vs. particle); magnitudes of ozone exposure; as well as the chemical species that are monitored: in coated-wall studies of uptake, ozone decay is monitored while in the AFT studies the loss of the condensed-phase OL is typically monitored. Experiments employing CFT have a long tradition and therefore will be described only briefly in this report.

2.1 Experiments with coatings and films

The CFT method has been adapted to organic solid and liquid coatings, as well as mono-layers (Rudich, 2003) and semi-solid coatings (Knopf et al., 2005). Typically, for liquid coating studies a wetted reactor is coated by placing a small volume of organic

11098

liquid within the reactor tube and rotating the reactor (de Gouw and Lovejoy, 1998; Moise and Rudich, 2000; Thornberry and Abbatt, 2004). With semi-solid coatings (Knopf et al., 2005), the preparative procedure affects the uptake of ozone as shall be discussed in detail later in this report. Ozone uptake is typically determined by monitoring the loss of O_3^- that is generated by chemical ionization with SF_6^- (de Gouw and Lovejoy, 1998; Knopf et al., 2005; Moise and Rudich, 2000; Thornberry and Abbatt, 2004; Hung et al., 2005; Hearn et al., 2005).

Another means of assaying the oxidative processing of organic films employs quartz crystal microbalances. This method has been used to study the effects of ozone exposure on thin films of OL, including the way that oxidation can affect water uptake (Asad et al., 2004). A good description of this methodology as it is applied to organic thin films has been given by Demou (Demou et al., 2003). In CFT studies, the films are exposed to variable relative humidity (RH) while the oscillation frequency of a piezoelectric oscillator balance is monitored. As shall be discussed, recent studies employing this method show that water uptake is dramatically enhanced with OL after ozone exposure.

2.2 Experiments with particles

To date, aerosol – ozone studies of OL that have focused on kinetics, mechanism and/or product evolution have utilized pure OL particles (Hearn et al., 2005; Hearn and Smith, 2004b; LaFranchi et al., 2004; Morris et al., 2002; Smith et al., 2002; Zahardis et al., 2005, 2006a; Ziemann, 2005), internally mixed particles containing OL (Hearn et al., 2005; Hearn and Smith, 2004b, 2005; Katrib et al., 2005a; Ziemann, 2005), and OL coatings on inert latex spheres (Katrib et al., 2004; Katrib et al., 2005b). Both monodisperse and polydisperse aerosols have been interrogated. Kinetic studies on particulate OL typically monitor its decay directly and correlate it with the uptake of ozone. The size range of OL particles (excluding particles with the morphology of an OL coating on latex spheres) employed in uptake studies ranges from about 200 nm to 2.45 μm , targeting particles in the accumulation mode of the fine range of atmospheric

11099

aerosols.

Motivation of OA studies in this size range include:

- The richness in organics of this range compared to that in the Aitken mode and in coarse particles (Hahn, 1980; Hoffman and Duce, 1977; Ketseridis and Eichmann, 1978)
- The great uncertainty in magnitude of the impact of fine OA on radiative effects, with the greatest uncertainty on CCN mediated indirect aerosol effects
- The choice of this size range is in accord with particle dimensions that may have greatest impact on human health

Most particle studies have employed AFT but environmental chambers have recently been used in the particle generation and reaction processes (Ziemann, 2005).

2.2.1 Aerodyne aerosol mass spectrometry

Morris et al. (2002) first employed an Aerodyne aerosol mass spectrometer (AMS) to study the OL- O_3 HRS (Morris et al., 2002). Numerous reports have appeared since on the use of the Aerodyne AMS to measure uptake of reactive gases (Katrib et al., 2005a; Morris et al., 2002), determine stoichiometry (Katrib et al., 2004; Morris et al., 2002), identify chemical products (Katrib et al., 2004), measure the volatility (Morris et al., 2002) of products formed by particles undergoing ozonolysis, observe changes in particle size (Katrib et al., 2005b) and morphology (Katrib et al., 2005a, b; Morris et al., 2002), and changes in particle density (Katrib et al., 2005b) due to ozonolysis. The Aerodyne AMS has been used to investigate particles with core-shell morphology (Katrib et al., 2004, 2005b) and has provided valuable information about changes in particle density, the O:C ratio and OL layer thickness as a function of ozone exposure.

2.2.2 Chemical ionization mass spectrometry

Chemical ionization mass spectrometry (CIMS) has been coupled to AFT-based experiments (Hearn et al., 2005; Hearn and Smith, 2004a, b, 2005) to measure the reactive uptake of ozone by OL, oleyl alcohol, linoleic acid, and 1-octadecene. Particles are entrained in a jacketed flow tube, exposed to ozone with the aerosol's velocity determined by light scattering (Hearn and Smith, 2004a, b). Reacted particles are vaporized by a heated tube and chemical ionization of the vapor phase species is by proton exchange. Little fragmentation occurs with this soft-ionization process. Other methods of chemical ionization have been employed in these studies (Hearn and Smith, 2004a, b). The direct detection of all the primary products of ozonolysis (azelaic acid, nonanal, nonanoic acid, and 9-oxononanoic acid) and HMW species was reported for the ozonolysis of OL as well as relative product yields of some of these products (Hearn and Smith, 2004b) (Table 1). CIMS has also been applied to the study of internally mixed particles (Hearn et al., 2005; Hearn and Smith, 2004b, 2005).

2.2.3 Single-particle mass spectrometry

Single-particle MS has shown applicability in the quantitative analysis of mixed particles, including OL and glycerol (Sykes et al., 2002), as well as measuring the uptake of ozone by OL (Smith et al., 2002). In these experiments, particles pass through an adjustable injector into a flow tube where they are reacted with ozone. Particle residence times are determined by light scattering. The OL decay is monitored by dual-laser, single-particle MS where an IR CO₂ laser evaporates single particles and vacuum ultraviolet radiation is used to ionize the resultant molecular vapor. This decoupled scheme for vaporization and ionization has been used successfully to minimize molecular fragmentation and simplify product identification (Smith et al., 2002; Woods III et al., 2001, 2002). The products observed and measured uptake coefficients of ozone by this method are summarized in Tables 1 and 2, respectively.

In a similar vein, experiments using synchrotron radiation in the vacuum ultraviolet

11101

range coupled with time-of-flight (TOF) are currently being adapted for real time analysis of OA including OL, and other FA (Mysak et al., 2005).

2.2.4 Photoelectron resonance capture ionization mass spectrometry

Photoelectron resonance capture ionization aerosol mass spectrometry (PERCI-AMS) (LaFranchi et al., 2004; Zahardis et al., 2005, 2006a, b) is a relatively new method to be applied to the OL-O₃ HRS. Again, aerosol is sampled into a flow tube where it is reacted with ozone. Particles are then sampled with an aerodynamic lens into the ionization region of MS, where they are deposited onto a resistively heated wire. The resulting vapor is ionized with low-energy electrons and the gas-phase anions are monitored by TOF MS (LaFranchi and Petrucci, 2004; LaFranchi et al., 2004). PERCI has been used for the direct and simultaneous measurement of all four of the primary products of the ozonolysis of OL (LaFranchi et al., 2004; Zahardis et al., 2005), HMW peroxidic species (Zahardis et al., 2005) including polymers (Zahardis et al., 2006a), and has been applied to mixed particles (Zahardis et al., 2006b). Some of these products are summarized in Table 1.

2.2.5 Thermal desorption particle beam mass spectrometry

The reactions of pure OL particles or mixed particles of OL and a second organic (for example, dioctyl sebacate (DOS), hexadecanoic acid (C16, palmitic acid), or heptadecanoic acid (C17)) have been studied in an environmental chamber using thermal desorption particle beam mass spectrometry (TDPBMS) (Ziemann, 2005). In these studies typically the OL is introduced by evaporation into an environmental chamber, after which particle formation proceeds via homogeneous nucleation. Mixed particles on the other hand are produced by nebulization of the appropriate solution. After reaction with ozone, the particles are analyzed in real-time by TDPBMS, collected and then vaporized by temperature programmed thermal desorption (TPTD) (Tobias and Ziemann, 1999), or their size distribution determined with a scanning mobility particle

11102

sizer, (SMPS). Vaporized particles are ionized by electron impact and mass analyzed by a quadrupole MS.

TDPBMS-TPTD has been utilized in measuring uptake of ozone by OL and mixed particles, elucidation of mechanism in the OL-O₃ HRS, and the observation of many products of ozonolysis of OL, including HMW peroxidic species (Ziemann, 2005). These results are summarized in Tables 1 and 2.

3 Pathways and products of ozonolysis of oleic acid

Ozonolysis is an oxidative reaction between ozone and the carbon-carbon double bond of an alkene. OL is an ideal model monounsaturated FA for studies of heterogeneous processing with ozone, being abundant and ubiquitous in the troposphere.

- It is the aim of researchers in this field to adapt the methods employed in the OL-O₃ HRS to more complicated organics and, importantly, multicomponent mixtures that reflect naturally occurring OA

A brief summary of ozonolysis is given below. While the emphasis of this review is on heterogeneous chemistry of tropospheric relevance, inference shall be drawn from solution reactions as well as gas-phase ozonolysis.

3.1 Overview of ozonolysis

Ozonolysis of an unsaturated compound is most simply described by a three step mechanism (Fig. 1) (Bailey and Ferrell, 1978; Criegee, 1975; Harding and Goddard III, 1978; Hiberty, 1976; Murray, 1968):

- **Step 1**) formation of a primary ozonide (PO)
- **Step 2**) decomposition of the PO to aldehydes (or ketones) and carbonyl oxides (or Criegee intermediates, CI)

11103

- **Step 3**) recombination of the carbonyl oxide and the aldehyde (or ketone) to form secondary ozonides (SO)

We will define the first two steps as the ‘primary steps’ of ozonolysis. In the ozonolysis of alkenes in bulk solution, particularly at low temperature, SO are often observed and have been isolated in high yield (Bailey, 1978). Similarly, in the heterogeneous ozonolysis of OL, a variety of highly-oxygenated products, including the SO (LaFranchi et al., 2004; Zahardis et al., 2005; Ziemann, 2005) and other peroxidic products, have been observed directly (Hung et al., 2005; Zahardis et al., 2005, 2006a; Ziemann, 2005) or inferred from kinetic data (Hearn et al., 2005).

- “Secondary chemistry” will be defined as the reactions of the CI and aldehydes that arise from decomposition of the PO, as well as any subsequent reactions of the products of the aforementioned reaction

CI are highly reactive and can react with each other, aldehydes, and other carbonyl or carboxyl group-containing species, including OL (Hearn et al., 2005; Hearn and Smith, 2004b; Hung et al., 2005; Katrib et al., 2005a; Zahardis et al., 2005, 2006a; Ziemann, 2005).

- Most of the secondary chemistry in the OL-O₃ HRS stems from the reactivity of the CI or from peroxidic products that arise from CI

The reactivity of the CI has long been noted in solution chemistry (Bailey, 1978; Harding and Goddard III, 1978). Some implications to OA, particularly mixed particles in which the organic medium can be viewed as the solvent, can be gleaned from solution chemistry:

- Product distributions (i.e. the types and/or relative yields of products) in solutions that are treated by ozonolysis often depend on the solvent (Bailey, 1978; Greenwood, 1945)

11104

- The presence and types of peroxidic products appears especially sensitive to the type of solvent (Bailey et al., 1974; Fliszár et al., 1966; Murray, 1968; Zelikman et al., 1971)
- Treatment of ozone-reacted mediums with acids (Bernatek et al., 1967; Bernatek and Ledaal, 1960) may decompose ozonides and cause the formation of peroxy-acids along with carbonyls. It is also well-established that bases can decompose ozonides and other peroxidic products of ozonolysis, forming ketones or aldehydes and carboxylic acids (Bailey, 1978). Ozonolysis in an aqueous medium can lead to the formation of α -alkoxyalkyl hydroperoxides (Bailey, 1978) and similar hydroperoxides, which may lead to the formation of aldehydes by further decomposition (Pryde et al., 1968; Sturrock et al., 1963).

In this report, emphasis will be placed on chemical products and yields in the OL-O₃ HRS as well as the uptake of ozone. There is apparent discord between predicted yields and what is observed experimentally. Experimental evidence strongly indicates that these anomalies arise from the reactivity of the CI. Furthermore, the reactivity of these CI may account, at least in part, for the variation in the measured uptake coefficient of ozone in this medium. Lastly, the products formed by the CI, including HMW oxygenates, may change the aerosol physical properties and have atmospheric implications, such as enhancing CCN ability. In light of these important factors, a brief introduction to the CI is in order and is given below.

3.2 Criegee intermediates

The reactivity of CI is of key importance to the types of products and their distributions in this HRS. Criegee showed solution-phase experimental evidence indicating CI were zwitterionic (Criegee, 1975) based on reactivity patterns (Criegee, 1975; Criegee and Wenner, 1949). On the other hand, as reviewed by Bunnelle (Bunnelle, 1991), other researchers presented computational evidence that CI were singlet biradicals (Goddard III et al., 1973; Wadt and Goddard III, 1975). Revised considerations of some early cal-

11105

culations (Harding and Goddard III, 1978; Wadt and Goddard III, 1975) indicated the energy difference between the biradical and zwitterionic forms of the smallest CI were artificially large. Most subsequent computational studies focus on simple CI. Semiempirical calculations have been employed to investigate the effects of larger substituents on the electronic structure of CI and mostly indicate that substituted CI have significant biradical character (Bunnelle, 1991). The distilling conclusion of these investigations is that the CI electronic structure is best represented as a resonance between the biradical and the zwitterion.

Recent investigations have focused on substituted CI in solution. Density functional theory calculations indicate that the dipolar character is enhanced by progressive methylation (Selçuki and Aviyente, 1998). Solvent effects and resonance have also been considered (Parrondo et al., 1995) and it has been indicated that zwitterionic character was enhanced with increasing dielectric constant of the solution.

- To our knowledge, no definitive calculation or measure of the CI electronic state of CI as heavy as these systems in the condensed-phase (9-carbon) exists to date.

In summary:

- CI have zwitterionic and biradical resonances
- Computational work to date has primarily focused on smaller CI
- We do not have an accurate description of the electronic state of CI generated in OL, let alone mixed OA. The electronic state of CI affects reactivity trends (Criegee, 1975; Criegee and Wenner, 1949); hence the predictions of product formation from ozonized OA will largely rely on empirical observations.

3.3 Primary products of the ozonolysis of oleic acid

There are four primary products anticipated from the decomposition of the PO of OL (Fig. 1): nonanal, 9-oxononanoic acid, and two CI, one the CI of azelaic acid and the

11106

other the CI of nonanoic acid. The latter two products are often described in the atmospheric research literature as simply azelaic acid and nonanoic acid, for it is usually assumed that the CI rearranges (at least in part) to the corresponding acid although this has not been verified and may be inaccurate.

- 5 – By the term *primary* product we do *not* explicitly mean major product because the product distributions in this system are in early stages of description and may be susceptible to reaction conditions

As shall be explained, at least one expert in this field shows results that the OL-O₃ HRS has peroxidic compounds as major products of ozonolysis under certain conditions (Ziemann, 2005).

10 The four primary products have been directly observed independently (Katrib et al., 2004; Moise and Rudich, 2002; Morris et al., 2002; Smith et al., 2002; Thornberry and Abbatt, 2004; Ziemann, 2005) and recently, by different groups, simultaneously by employing a variety of methodologies (Hearn and Smith, 2004b; Hung et al., 2005; 15 LaFranchi et al., 2004). The yields of these products have been measured by some researchers and a recent compilation (Hung et al., 2005) of the relative yields and observed products is given in Table 1.

- Anomalies exist in the relative yields of these products as measured to date

As shown in Fig. 1, the PO formed in the first step of ozonolysis of OL has two distinct 20 routes (*ac* and *bc*) of decomposition. In the case of the PO of OL, the distal position of the carboxylic acid group to the peroxidic bond should be far enough not to influence (significantly) the decomposition route, hence the expected relative yield (to OL) for each of the products is 0.5 (moles of each product per mole of OL consumed) (Hearn and Smith, 2004b).

11107

3.3.1 Azelaic acid

Azelaic acid, along with nonanal, are the *ac*-cleavage products of the second step of ozonolysis. Azelaic acid has been independently measured at 6% by Hearn and Smith (2004b) and Hung et al. (2005) on the carbon-based yield scale (Hung et al., 2005). As 5 summarized in Table 1, Hearn and Smith used CIMS to assay polydisperse aerosols with a mean diameter of 800 nm, while Hung et al. oxidized OL as sub-millimeter to mm diameter droplets. Hung et al. had only a slightly larger number density of ozone compared to Hearn et al., but a much higher exposure due to the long time the droplets were exposed to the oxidant.

10 The yield of azelaic acid was also quantified by Katrib and coworkers in their studies of particles with core-shell morphology (Katrib et al., 2004) using an Aerodyne AMS. The yield was between 1–3% on the carbon-based yield scale for coatings between 2–30 nm in thickness. There appears to be a slight increase in azelaic acid yield with increasing thickness of OL.

15 As summarized on Table 1, other groups have detected, but not quantified, azelaic acid in the OL-O₃ HRS using AFT, CFT, and environmental chambers.

- It should be noted that azelaic acid is described in the current literature as arising from the rearrangement of the CI that stems from the *ac*-route cleavage of OL (Hearn and Smith, 2004b; Katrib et al., 2004; Moise and Rudich, 2002; Rebrovic, 1992; Thornberry and Abbatt, 2004; Zahardis et al., 2005). It has not, to our 20 knowledge, been rigorously shown that the observable signal in the mass spectrum does not arise, at least in part, from a stabilized CI directly. *For brevity*, in accord with the terminology of the original authors, we shall refer to these signals as arising from the CI rearrangement product (i.e. the acid) and not the stabilized CI itself. 25

11108

3.3.2 Nonanal

Nonanal, which is the other product of the second step of ozonolysis by the *ac*-route cleavage, is the most volatile of the four primary products. In many cases, especially with the AFT based methodologies, this high volatility makes it difficult to measure nonanal. As shown in Table 1, Hearn and Smith (Hearn and Smith, 2004b) have measured a yield of 42% for this product on the carbon-based yield scale, with details provided by the authors of how they accounted for volatility losses. The authors assume that the two *ac*-route products, azelaic acid and nonanal, are detected with equal efficiencies and a sum of moles of the products per mole of OL of this route is unity. The authors note that caution should be taken with these values since they are based on rather broad assumptions.

Hung and coworkers (Hung et al., 2005) reported a 30% yield of nonanal on the carbon-based yield scale with their studies of OL droplets. This yield accounted for only nonanal in the condensed-phase, as opposed to Hearn and Smith, whose measure accounted for both the condensed and gas-phase nonanal. Furthermore, Hung and coworkers reported that $48 \pm 5\%$ of the carbon was not detected. Indeed, the volatility of this species may be the cause for this discrepancy. Loss of nonanal by evaporation is in accord with the considerable loss of particulate mass measured in their experiments – upwards of 30% by carbon number. The radii of the droplets used by Hung et al. and the particles of OL used by Hearn and Smith were much larger than the coating thickness used by Katrib et al., which may account for the apparent anomaly in nonanal yield.

CFT based methods have also been used to quantify the nonanal yield and studies to date report carbon-based yields of 25% (Moise and Rudich, 2002; Thornberry and Abbatt, 2004). Thornberry and Abbatt detected the aldehyde product using CIMS with proton-transfer from H_3O^+ (Thornberry and Abbatt, 2004). Only gas-phase species were detected in this study so no comparison to the yield of azelaic acid is possible. The authors note that the high volatility of nonanal caused some irreproducibility in their calibrations (Thornberry and Abbatt, 2004). A nonanal yield was reported by Moise

11109

and Rudich, with details of the mass spectral assignments given in the original article (Moise and Rudich, 2002) and details of the conditions given on Table 1. The yield of this aldehyde seems to be a function of temperature, with the yield decreasing from 296 K to 279 K with all other experimental conditions identical. Interestingly, the yield increases again if the temperature is decreased further (i.e., below 279 K). Similar behavior was observed with LA. A more detailed description of these temperature effects is beyond the scope of this report. Readers interested in the temperature dependency of product evolution, ozone consumption, and its uptake by OL and related organic liquids, solids, and monolayers should consult the original works on these coated-wall reactor experiments (de Gouw and Lovejoy, 1998; Moise and Rudich, 2000, 2002; Thornberry and Abbatt, 2004).

In summary:

- The yield of nonanal is difficult to quantify due to volatilization losses
 - Yields vary considerably between experiments probably due to differences in sizes of particles and droplets and thicknesses of coatings. Yields may be a function of temperature
 - When detected, the yield of nonanal is relatively high compared to azelaic acid, which is not expected because both products originate from the same decomposition route (i.e., *ac*-cleavage)
- These observations seem to imply that
- The high relative yield of nonanal to azelaic acid is probably due to secondary chemistry of the CI associated with the latter species

3.3.3 Nonanoic acid

Nonanoic and 9-oxonanoic acid are the *bc*-cleavage products of the second step of ozonolysis. The yield of nonanoic acid has been quantified at 7% for droplets (Hung

11110

et al., 2005) and 9% particles (Hearn and Smith, 2004b) and 2% for coated particles (Katrib et al., 2004), all values adjusted to the carbon-normalized scale. Hearn and Smith (2004b) used aerosol CIMS; however, for this particular measure the reaction was performed offline, complicating comparison of yields from different routes. As summarized in Table 1, nonanoic has been detected in several other AFT experiments and in at least one CFT experiment, but in these cases the yield was not quantified.

- As with azelaic acid, it has not been considered whether part of the observable signal in the mass spectrum does not arise, at least in part, from a stabilized CI directly

10 3.3.4 9-oxononanoic acid

The other *bc*-route product, 9-oxononanoic acid, shows a large yield relative to nonanoic acid (Hearn and Smith, 2004b; Hung et al., 2005; Katrib et al., 2004). Hearn and Smith (2004b) report a carbon-normalized yield of 42%, while Hung et al. (Hung et al., 2005) report a yield of 14% from their OL droplet experiments after a relatively long exposure time of 2000 s. This product yield increases with ozone exposure as shown in the original work (Hung et al., 2005). Katrib and coworkers (Katrib et al., 2004) report a 35% yield of 9-oxononanoic acid for 30 nm coatings of OL. As summarized in Table 1, 9-oxononanoic acid has been detected by other AFT and at least one CFT experiment but not quantified. It was also reported in environmental chamber experiments coupled to TDPBMS (Ziemann, 2005), though the yield was not quantified.

A conclusion that can be drawn for these results is that

- The high yield of 9-oxononanoic acid relative to nonanoic acid may be explained by losses of the CI associated with nonanoic acid through secondary chemical pathways

11111

3.4 Secondary products of the ozonolysis of oleic acid

The consistently lower yield of the acids arising from CI compared to their partners from a cleavage route likely arises from the high reactivity of the CI. This reactivity has been attributed to a host of oxidized products including ketones, and peroxide products.

5 3.4.1 Ketones

One of the first products of secondary chemistry reported in the OL-O₃ HRS was 9-oxooctadecanoic acid (OOA) (298 u) (Hearn and Smith, 2004b). This product was proposed to have been formed by the addition of the CI to the double bond of OL, which subsequently decomposes to OOA and either 9-oxononanoic acid or nonanal – both of which, when quantified, are reported to be of relatively high yield compared to their decomposition route partner (Hearn and Smith, 2004b; Hung et al., 2005; Katrib et al., 2004). A mechanism for this type of reaction had been proposed originally by Katrib et al. (2004), although the secondary product was not directly detected. Zahardis et al., have reported this product as detected by PERCI-AMS (Zahardis et al., 2006a). Follow-up studies with related FA and methyl esters (Zahardis et al., 2006b) showed that stearic acid, which is the saturated analogue of OL, did not undergo similar oxygenation when undergoing ozonolysis. Also the saturated methyl ester, methyl palmitate, showed no oxygenation after ozonolysis, while unsaturated methyl esters showed evidence of oxygenation.

- Ketones may be formed as secondary products of ozonolysis via secondary reaction of a CI

3.4.2 Peroxides and hydroperoxides

The formation of peroxides, including hydroperoxides, is an important feature in the secondary chemistry of the OL-O₃ HRS. This is not surprising, having long been noted in solution chemistry that CI can undergo dipolar cycloaddition with aldehydes and

11112

other CI forming SO and geminal diperoxides, respectively (Bailey, 1978; Criegee, 1975; Murray, 1968). An extensive compilation of this type of secondary chemistry is given elsewhere (Bailey, 1978)

SO can be formed by two main routes: a) the dipolar cycloaddition of the CI and the aldehyde that originate from the same route of decomposition of the PO; and, b) the dipolar cycloaddition of the CI and the aldehyde from opposite decomposition routes (Criegee, 1975). (Here we are ignoring the reaction with an aldehyde from an external source.) For simplicity, the former shall be referred to as the "conventional" SO and the latter as the "cross" SO, because the former appears to be the predominant type of SO formed in most studies in solution phase (Murray, 1968; Murray and Williams, 1969). Three geminal diperoxides are possible, two by the "conventional" route and one by "cross" cycloaddition. Two of these species were identified by Zahardis et al. (2005), with similarly weak signal intensity, though not quantified.

Recent work (Zahardis et al., 2005; Ziemann, 2005) suggests that organic peroxides may be a significant contributor to the OL-O₃ HRS. In one study it was estimated that the organic peroxides comprised 68% of the total aerosol product mass, while 9-oxononanoic acid and azelaic acid were, respectively, only 28 and 4% (Ziemann, 2005). The classes of peroxidic products that have been measured include: α -acyloxyalkyl hydroperoxides (ACOAH), SO, α -alkyloxyalkyl hydroperoxides (ALOAH), and oxocarboxylic acids. Figure 2 gives some illustrative examples of the reactions leading to some of these types of products. One of the assigned ACOAH was proposed to be formed from either the reaction of 9-oxononanoic acid with a secondary CI or from an SO with the acid moiety of OL followed by oxidative cleavage about the double bond (Ziemann, 2005). The reactivity of ACOAH has also been demonstrated by addition of octanal to the OL-O₃ HRS after ozonolysis (Ziemann, 2005). This led to the formation of a peroxyhemiacetal, which further reacted with 9-oxononanoic to form an observed bis (α -acyloxy- α -alkyl) peroxide. Finally, the high degree of functionality of many of the measured reaction products implies the existence of numerous pathways leading to the formation of HMW products or oligomers. The very recent observations

11113

of polymerization in this system shall be discussed in the next section.

Some notable points regarding the richness of the secondary chemistry in the OL-O₃ HRS include

- The yield of peroxidic products may be higher than expected in this HRS
- There are a variety of different reactions that can lead to peroxides, which can react further
- Generally the products that form are HMW, low volatility, hydrophilic and increase the O:C ratio of the particulate

This implies

- Oxidative processing of OA that has unsaturated constituents, may show considerable peroxide formation that may enhance CCN ability

3.4.3 Polymers

Hung et al. (2005) have studied the reactions of mm-sized droplets of OL with ozone and a number of products observed by IR indicated the presence of ester groups. These HMW products were separated by masses corresponding to 9-oxononanoic acid and the azelaic acid CI, which, by their description, acted as polymerization propagators. This polymerization is in their description quite general, the CI adding to OL, carboxylic acids, or aldehydes. The authors also depict other novel polymers that contain both ACOAH motifs and SO moieties on the same polymeric backbone. There was also a discernable increase in viscosity of these droplets that could be attributed to the HMW polymers formed during ozonolysis. Zahardis and coworkers (Zahardis et al., 2006a) also observed polymer formation in the OL-O₃ HRS, with a series of products differing by 170 u suggesting polymerization by a similar mechanism, namely the addition of an in situ generated CI to the carboxyl group of OL forming an ACOAH (Fig. 3).

11114

Polymerization of OL has also been observed in thin films (Asad et al., 2004), noting a concomitant increase in water uptake to OL film exposure to ozone. Chemical changes were monitored in the thin films by IR spectroscopy, with broad absorption features in the exposed film that “probably correspond to OH stretching transitions of the polymeric species and associated carboxylic acids, respectively” (Asad et al., 2004). By direct comparison to the IR spectrum of azelaic acid, Asad et al. (2004) concluded this species was *not* present in the condensed-phase and that the reacted medium was “a substance or mixture which was much more highly oxidized”.

In summary

- The formation of highly oxygenated, HMW, low volatility peroxide polymers can arise from the CI generated in ozonolysis

The implications of these results are that

- The observation of HMW, low volatility species in tropospheric OA in part may be polymeric material formed from ozone exposure
- The presence of highly oxygenated polymers in tropospheric OA would likely increase their CCN ability

3.4.4 Background support of organic peroxide formation

In Bailey’s compilation (Bailey, 1978) on ozonolysis, many of the classes of peroxides discussed are shown to be prevalent in protic, nucleophilic solvents. A number of peroxidic products have been reported for the ozonolysis of unsaturated FA, including a 1-acyloxyalkyl-1-hydroperoxide, a SO and a bis(1-acyloxy- α -alkyl) peroxide, by sparging solutions of the FA with ozone (Ledea et al., 2003; Nishikawa et al., 1995; Pryde et al., 1968; Rebrovic, 1992).

In the gas-phase, peroxide formation, notably hydroperoxides, has been observed in the ozonolysis of simple alkenes, including the ethene-ozone homogenous reaction system (E-O₃ RS) (Fenske et al., 2000; Horie et al., 1994; Neeb et al., 1995, 1996,

11115

1998; Wolff et al., 1997) and other systems (Baker et al., 2001; Fenske et al., 2000; Gutbrod et al., 1997). The types of products formed may be a function of reaction conditions, including RH. For example, methyl hydroperoxide has been observed in the dry ozonolysis of ethene, while under wet conditions this species along with hydroxymethyl hydroperoxide were observed (Horie et al., 1994). The formation of these hydroperoxides involves reactions of CI. A good comparison of gas and liquid-phase ozonolysis of ethene, including the formation of peroxidic products, is given by Neeb and coworkers (Neeb et al., 1998).

Ozonolysis of both gas and liquid-phase alkenes in the presence of alcohols (Tobias and Ziemann, 2000, 2001; Ziemann, 2003), aldehydes (Tobias and Ziemann, 2001), water (Tobias et al., 2000; Tobias and Ziemann, 2001), and acids (Tobias and Ziemann, 2000, 2001) can lead to the formation of peroxides (ozonides, hydroperoxides, peroxyhemiacetals, etc) and may lead to secondary organic aerosol (SOA) formation under some conditions (Tobias et al., 2000; Tobias and Ziemann, 2000, 2001; Ziemann, 2003). For example, two major products have been identified for each 1-tetradecene-O₃ system (T-O₃ S) in the presence of an alcohol and an acid. One class of compounds was relatively more volatile, namely α -alkoxytridecyl or α -acyloxytridecyl hydroperoxides. The relatively less volatile class consisted of α -alkoxy- α' -hydroxyditridecyl or α -acyloxy- α' -hydroxyditridecyl peroxides (i.e. peroxyhemiacetals) (Tobias and Ziemann, 2000).

- Diverse secondary reactions are possible with the ozonolysis of simple alkenes, especially in the presence of additive species: water, acids, aldehydes, alcohols

T-O₃ S yields tridecanal, which reacts with in situ generated hydroperoxides forming peroxyhemiacetals (Tobias et al., 2000). Figure 2 shows a similar reaction between an ACOAH and an aldehyde giving a peroxyhemiacetal. An extensive list of assigned organic peroxides arising in the T-O₃ S has been given by Tobias et al. (2000).

Further studies on the T-O₃ S noted the effects of humidity on the chemical speciation of the reaction products (Tobias et al., 2000). Humid air favored α -hydroxytridecyl

11116

hydroperoxides and bis (α -hydroxytridecyl) peroxides, whereas dry air favored SO.

In summary,

- HMW oxygenates with low vapor pressure can be formed from the ozonolysis of simple alkenes and these products vary in the presence of water and other species ubiquitous to the natural troposphere
- The presence of these low vapor pressure products ($<10^{-6}$ torr) (Tobias and Ziemann, 2000) can enhance SOA formation, aerosol growth and nucleation

4 Reactive uptake of ozone: overview

Atmospheric heterogeneous processing can be described as the transformation of one species on or close to a particulate's surface. Although this review focuses on the ozonolysis of OA, with emphasis on OL, much of the framework for describing heterogeneous processing comes from considerations of inorganic aerosols (namely water and sulfate) with trace gases. Much of the early work in this regard focused on the uptake of halogenated species by sulfuric acid aerosols (Abbatt and Nowak, 1997; Donaldson et al., 1997; Hanson, 1998; Hanson and Lovejoy, 1995; Hanson and Ravishankara, 1993; Hanson et al., 1996). The models developed for describing inorganic HRS were adapted to the uptake model used for OL and other organics.

Understanding uptake of ozone is central to describing the processing of OA and in the Discussion we will address the tropospheric implications based on insight gained from the OL-O₃ HRS. These implications address broad questions in regards to tropospheric chemistry:

- How does OA compare to organic gas-phases as a significant sink of ozone?
- How is the lifetime of an unsaturated species in OA affected by ozonolysis? Furthermore, how is this lifetime affected in real OA with many components and the possibility of different phases and phase separation?

11117

- How does oxidative processing, such as ozonolysis of OA, enhance the CCN ability of the OA and subsequently affect the global radiative budget?
- How does the formation of aldehydic products by the ozonolysis of OA contribute to the oxidizing capacity of the troposphere?

The aim of this review is to provide consolidated information on an important model HRS, with focus on the products, secondary chemistry, and the reactive uptake of ozone such that workers in the field, theorists, and those in the laboratory can better approach some of the questions regarding OA.

4.1 Models of reactive uptake

The formalism developed by Worsnop et al. (2002) adapts the model of uptake of gaseous species by liquids (Davidovits et al., 1991; Hanson, 1997; Hanson and Lovejoy, 1995; Kolb et al., 2002; Shi et al., 1999) to reactive transforms of the condensed-phase organic species because the particle MS methods monitor the loss of the organic substrate. In the OL-O₃ HRS, this involves monitoring OL loss and using this loss to calculate the uptake coefficient, γ . We shall discuss and present uptake data garnered from AFT and CFT experiments, the latter of which typically monitor the loss of ozone. The latter method is well-established with a long tradition, hence we will only give the results employing this method and the interested reader is referred to the literature for details on the kinetics formalism (Lovejoy et al., 1995; Moise and Rudich, 2000; Thornberry and Abbatt, 2004; Utter et al., 1992).

We shall provide a summary of the formalism developed by Worsnop and coworkers and others in regards to reactive uptake. Complete descriptions including the formal derivations are available to interested readers (Hearn et al., 2005; Smith et al., 2002; Worsnop et al., 2002). Figure 4 illustrates the key parameters invoked in the uptake of a trace gas by OL as it is described to date. One of the key parameters is the mass accommodation coefficient, α , which is the probability of the trace gas entering the

11118

particle-phase:

$$\alpha = \frac{\# \text{ molecules entering particle phase}}{\# \text{ molecules that collide with surface}} \quad (1)$$

As described by Worsnop et al. (2002), in the absence of surface reactions the mass accommodation is directly proportional to the flux, J_x , of the trace gas, x , into the liquid

$$J_x = \frac{n_x \bar{c} \alpha}{4} \quad (2)$$

where n_x is the number density of gas-phase ozone molecules (cm^{-3}) and \bar{c} is the mean thermal velocity (cm s^{-1}) of gas-phase ozone. Equation (2) is valid only when the trace gas has no surface reaction with other gaseous molecules at the surface, itself, or with the liquid-phase species.

In equilibrium systems there is no net uptake of the trace gas by the liquid. However, reactions of the solvated trace gas can act as a sink for that gaseous species and the flux is now proportional to the uptake coefficient, γ :

$$J_x = \frac{n_x \bar{c} \gamma}{4} \quad (3)$$

The uptake coefficient is less than or equal to unity since the flux must be less than or equal to the collision frequency of the gas with the surface. In considering the OL- O_3 HRS, it can be shown readily that the particle-phase OL loss is given by:

$$-\frac{d[\text{OL}]}{dt} = \frac{3 n_x \bar{c} \gamma}{4 a} \quad (4)$$

where "a" is the particle radius and the ratio of 3 to 4a accounts for the surface to volume ratio of the particle. Analytical solutions to Eq. (4) are not known (Worsnop et al., 2002), so analysis proceeds by considering limiting regimes in a fashion developed by Crank (Crank, 1975) and Danckwerts (Danckwerts, 1970).

11119

4.2 The resistor model

A model has been developed that attempts to decouple the measured uptake coefficient, γ_{meas} , into constituent chemical and physical processes (Fig. 4) including gas- and particle-phase diffusion (Γ_{diff} and Γ_{diff}^p , respectively), mass accommodation (α), bulk solubility (S) and reactivity term(s) (Γ_{rxn}) (Worsnop et al., 2002).

The loss of ozone to the particle can be described by Fick's second law, accounting for the chemical reactivity with the $k[\text{O}_3]$ term in Eq. (5), which is an expression for ozone loss:

$$-\frac{\partial[\text{O}_3]}{\partial t} = -D \nabla^2[\text{O}_3] + k[\text{O}_3] \quad (5)$$

The pseudo-first order approximation is evoked with $k=k_2[\text{OL}]$. This approximation requires that the OL diffuse rapidly to the surface (or near-surface region) and replenishes all the reacted substrate quickly. The steady-state approximation is typically evoked (i.e., $\partial[\text{O}_3]/\partial t=0$), and, assuming only a radial dependency of $[\text{O}_3]$, gives

$$D \nabla^2[\text{O}_3] = k[\text{O}_3], \text{ with } \nabla^2 = \frac{1}{r^2} \frac{\partial}{\partial r} \left(r^2 \frac{\partial}{\partial r} \right) \quad (6)$$

It has been shown (Smith et al., 2002) that applying finite ozone boundary conditions at the origin and assuming its concentration at the surface to be constant that

$$[\text{O}_3] = \frac{H P_{\text{O}_3} a \sinh(r/l)}{r \sinh(a/l)} \quad (7)$$

In Eq. (7) H is Henry's law constant and l is the diffuso-reactive length and is effectively the length the ozone must diffuse into the particle to react. P_{O_3} is the pressure of ozone (atm). The diffuso-reactive length is given by

$$l = \left(\frac{D}{k} \right)^{1/2} \quad (8)$$

11120

where D is the diffusion coefficient of ozone in the reactive matrix ($\text{cm}^2 \text{s}^{-1}$) and k is the pseudo-first order rate constant (s^{-1}). The gradient and the flux of ozone through the gas-particle boundary can be derived from Eq. (7) (Smith et al., 2002) and normalization of the surface flux to the collision frequency with the surface, gives the uptake coefficient. Substitution of the uptake coefficient into Eq. (4) is used to derive a rate of change of OL in terms of key parameters and variables:

$$\frac{d[\text{OL}]}{dt} = \left(\frac{-3 P_{\text{O}_3} H(k_2 D [\text{OL}]^{1/2})}{a} \right) \left[\coth \left(a \left(\frac{k_2 [\text{OL}]}{D} \right)^{1/2} \right) - \frac{1}{a} \left(\frac{D}{k_2 [\text{OL}]} \right)^{1/2} \right] \quad (9)$$

No general solution is known for Eq. (9); however, solutions have been found in four limiting regimes. These solutions have been derived previously (Smith et al., 2002; Worsnop et al., 2002) and we only present an outline of the methodology and physical assumptions.

4.3 Limiting cases of reactive uptake

The solutions to Eq. (9) for the four limiting regimes are summarized in Table 3 in terms of the ratio $[\text{OL}]/[\text{OL}]_{t=0}$, since particle-based methods measure the concentration of condensed-phase OL prior to and post reaction with ozone. In summary, these cases are:

- **Case 1: Rapid diffusion of ozone throughout the particle.** In this case $l > a$ and the right hand factor in Eq. (9) is approximately equal to $a/3l$ when $a/l < 1$ (Smith et al., 2002)
- **Case 2: Reaction limited by ozone diffusion or a near surface reaction.** In this case $l < a/20$, and in Eq. (9) the factor $[\coth(a/l) - a/l]$ approaches unity (Smith et al., 2002)

11121

- **Case 3: Reaction at the surface.** This assumes the reaction of OL and ozone is at the surface and second order (Smith et al., 2002), with δ being the surface depth
- **Case 4: Uptake limited by OL diffusion.** Notice in this case D_{OL} is the diffusion coefficient of OL and should not be confused with D , which is the diffusion coefficient of ozone in OL (Worsnop et al., 2002)

4.4 Experimental determination of reactive uptake

This section will begin with a summary of experiments that place emphasis on the measured uptake of ozone by OL, with the results of coated-wall studies presented first, and then the AFT studies. Secondly, the results from studies on related FA, internally mixed particles containing OL and/or other FA, and some other related organics will be presented. Emphasis will be placed on noting the approximations utilized in calculating the uptake coefficient, and all kinetic information that gives insight into the extent of secondary chemistry in these systems.

4.4.1 Reactive uptake: one-component coatings

Early measurements of the uptake of ozone by organic liquids on coated-wall reactors were performed by de Gouw and Lovejoy (de Gouw and Lovejoy, 1998). They measured the reactive probability (i.e. uptake coefficient) of ozone by a variety of organic liquids including canola oil, which is predominately OL (Mag, 1990). Employing a rotating wetted-wall reactor they determined an uptake coefficient of $\sim 8 \times 10^{-4}$. (A complete list of numerical values of reactive probability as a function of temperature was not provided in the original work; we estimated this value for $\sim 25^\circ\text{C}$ by interpolation from the plot provided in the original work.)

Moise and Rudich (2002) employed a rotating wall flow reactor to measure uptake coefficients for liquid and frozen OL of $(8.3 \pm 0.2) \times 10^{-4}$ and $(5.2 \pm 0.1) \times 10^{-5}$, respectively. The uptake coefficient for liquid-phase OL is in good agreement with the value

11122

of de Gouw and Lovejoy's (1998) for canola oil, despite the fact that most of the OL in canola oil is in the form of triacylglycerols (Mag, 1990). Comparable measurements were performed on LA, with the liquid and frozen phases having uptake coefficients of $(1.2 \pm 0.2) \times 10^{-3}$ and $(1.4 \pm 0.1) \times 10^{-4}$, respectively. LA has a considerably larger uptake coefficient compared to OL because the molecule contains two sites of unsaturation, effectively giving it twice the reactive capacity of OL.

Moise and Rudich (2002) suggested that for the liquid-phases the reaction in the bulk of the medium may contribute significantly to the uptake of ozone. This suggestion was based in part on previous observations of uptake of ozone by alkenes and other reaction systems (Moise and Rudich, 2002; Moise et al., 2002) and similar conclusions could be drawn from studies employing monolayers and bulk liquids (Moise and Rudich, 2000).

As noted by Moise and Rudich (2002) for the liquid FA, if the reactivity towards ozone is proportional to the FA concentration and each carbon-carbon double bond reacts independently, then the ratio, R , of uptake coefficients of OL to LA is given by

$$R = \sqrt{\frac{2 \times \rho_{LA} \times MW_{OL}}{\rho_{OL} \times MW_{LA}}} \quad (10)$$

with ρ denoting the density (g cm^{-3}) of the respective FA. The theoretical value of R in this case is 1.43. The experimental value calculated by Moise and Rudich (2002) for the liquids is 1.45 ± 0.19 , which lead the authors to conclude that "the reactant activity is directly related to the concentration of double bonds, supporting the conclusion that the uptake has a dominant contribution from reaction in bulk" (Moise and Rudich, 2002).

Thornberry and Abbatt (2004) investigated the uptake of ozone by liquid-phase OL, LA and linolenic acid (LN), in coated-wall tube experiments. In regards to OL and LA, their results were in accord with those of Moise and Rudich (2002); the uptake coefficient of ozone for OL was $(8.0 \pm 1.0) \times 10^{-4}$, for LA $(1.3 \pm 0.1) \times 10^{-3}$, and for LN $(1.8 \pm 0.2) \times 10^{-3}$. Again, the correlation between the uptake coefficient and degree of unsaturation is evident.

11123

Key conclusions from these experiments are

- γ has a value $\sim 8 \times 10^{-4}$ for the OL-O₃ HRS
- γ increases with degree of unsaturation
- The limiting case regime is probably Case 2 and/or 3

4.4.2 Reactive uptake of ozone by one-component particles

Since 2002, the results dedicated to the online analysis of the uptake of ozone by OL and other FA particulate have been presented to the atmospheric community. These methods include Aerodyne AMS, single-particle MS, CIMS, and TDPBMS and have directly monitored decay of the condensed-phase species (i.e. OL) to calculate the uptake coefficient of ozone. These new methods aim to monitor the reactions of condensed-phase species and determine γ from their decay; however, since γ is not measured by monitoring the decay of ozone directly, these results should initially be compared with those of coated-wall reactor methods.

4.4.2.1 Reactive uptake: Aerodyne Aerosol Mass Spectrometry

The Aerodyne AMS methodology has been applied to study the uptake of ozone by size-selected particles of OL (Morris et al., 2002). Based on the measured gas-phase diffusion uptake coefficient (0.30 to 2.0) compared to the uptake coefficient determined by others ($\sim 10^{-3}$), the authors used Case 2 as the limiting regime. They calculated the diffusive-reactive length, l , to be approximately 5 nm by equation Eq. (8), using $D \sim 10^{-6} \text{ cm}^2 \text{ s}^{-1}$ and $k_2 \sim 10^6 \text{ M}^{-1} \text{ s}^{-1}$ and treating [OL] as the initial concentration of OL, 3.15 M. The radius of the OL particle was assumed constant, and the product $P_{O_3} t$ was taken as an experimental variable. The curves were then fit by adjusting two parameters: $H (Dk_2)^{1/2}$ and τ . (The latter is a correction for the mixing time of ozone

11124

into the particle beam; Morris et al., 2002) and an uptake coefficient of $(1.6 \pm 0.2) \times 10^{-3}$ was calculated for a maximum O_3 exposure of $\sim 10^{-4}$ atm s.

4.4.2.2 Reactive uptake: single-particle mass spectrometry

The uptake of ozone has also been measured by single-particle MS (Smith et al., 2002) with particles from 680 nm to 2.45 μm in diameter. The diffuso-reactive length was estimated to be 20 nm as described previously, with the only difference in the calculation being the diffusion constant of ozone in OL, which in this case was estimated to be $10^{-5} \text{ cm}^2 \text{ s}^{-1}$ (as opposed to $10^{-6} \text{ cm}^2 \text{ s}^{-1}$). Figure 5 shows decay curves of OL determined by this method. Two limiting cases of reactive uptake, namely Cases 2 and 3, were suggested and as noted by the authors “it is possible that the O_3 reacts at both the surface and the bulk of the particle, but it is difficult to estimate the relative contributions of the two cases without accurate knowledge of k_2 , k_2^{surf} , H and D .” The authors noted further that Case 2 fit the data better when all particle sizes were considered and was used for the calculations with $H (Dk_2)^{1/2}$ estimated as previously described. The uptake coefficient ranged from $(0.99 \pm 0.09) \times 10^{-3}$ to $(7.3 \pm 1.5) \times 10^{-3}$ for particles ranging, respectively, from 2.45 μm to 680 nm with a maximum ozone exposure on the order of 10^{-3} atm s.

Careful consideration of the data in Fig. 5 shows an anomaly noted by the authors: although Case 2 has no explicit dependency of γ on the particle radius, there is a clear linear dependence when γ is plotted as a function of the particle radius. The authors acknowledge that the model does provide a good fit for the data; however “(the model) does not describe our data adequately” (Smith et al., 2002). The authors suggest the decrease in γ with increasing particle radius may stem from the diffusion of OL, with this effect more pronounced in larger particles. The authors estimated that the value of the uptake coefficient would be about $(5.8\text{--}9.8) \times 10^{-3}$ for small particles, where this OL diffusion is not the limiting factor in uptake. They then numerically solved a coupled set of reaction-diffusion equations for $[O_3]$ and $[OL]$, without making the steady-state

11125

assumption for ozone or assuming rapid diffusion of OL. The value of the self-diffusion constant of OL, D_{OL} , was varied and it was found that Case 2 was applicable when $D_{OL} = 3 \times 10^{-7} \text{ cm}^2 \text{ s}^{-1}$. It was reasoned that as ozonolysis of OL proceeds, the formation of reaction products and the loss of OL near the surface may slow the diffusion of OL to that region. They found that only by lowering the value D_{OL} to between $(4\text{--}10) \times 10^{-10} \text{ cm}^2 \text{ s}^{-1}$, as a function of the particle size, could they fit the numerical solutions for $[OL]$ to all their experimental data (Smith et al., 2002).

In summary

- The value of γ is dependent on particle radius with values of $(0.99 \pm 0.09) \times 10^{-3}$ to $(7.3 \pm 1.5) \times 10^{-3}$ for particles ranging, respectively, from 2.45 μm to 680 nm in diameter
- OL diffuses more slowly in the particles than is predicted by its self-diffusion coefficient

This suggests

- The formation of other HMW products, such as polymers, from ozonolysis, which can have a considerable effect on subsequent uptake

4.4.2.3 Reactive uptake: chemical ionization mass spectrometry

Hearn and Smith applied aerosol CIMS methodology to polydisperse particles of OL (Hearn and Smith, 2004b). In light of previous results (Moise and Rudich, 2002; Morris et al., 2002; Smith et al., 2002), they assumed kinetics governed by the limiting Case 2. The polydisperse OL decay data was fit in a similar fashion as described previously. The best fit of γ for polydisperse OL with an average diameter of 800 nm was $(7.5 \pm 1.2) \times 10^{-4}$. Polydisperse particles with other average diameters, namely 1.20 and 1.50 μm were assayed with γ determined to be 7.2×10^{-4} and 7.3×10^{-4} , respectively. The authors noted that their results were in good agreement with those from coated-wall experiments (Moise and Rudich, 2002; Thornberry and Abbatt, 2004) but were

11126

lower than the results for the other two previously mentioned aerosol-based methods (Morris et al., 2002; Smith et al., 2002).

By a similar method, Hearn and Smith (2004b) determined the uptake coefficient of polydisperse LA with a mean diameter of 800 nm to be $(1.1 \pm 0.2) \times 10^{-3}$. Two other single component polydisperse particles were studied: oleyl alcohol and 1-octadecene (Hearn and Smith, 2004b). The former is the alcohol analogue of OL and had the identical value for the uptake coefficient as OL: 7.5×10^{-4} for particles with an 800 nm average diameter. The value of γ for 1-octadecene was considerably smaller than that of OL, only 2.4×10^{-4} for polydisperse particles with an 800 nm average diameter, possibly due to the position of the double bond, or inhibited solubility or diffusion of ozone within the alkene (Hearn and Smith, 2004b).

In summary

- CIMS gave a value of $\sim 7 \times 10^{-4}$ for polydisperse OL particles assuming Case 2, a value in better agreement with coated-wall reactor measures than other particle based methods
- This method appears very convenient for measuring polydisperse particles, but the radial dependency on γ is not readily extracted

Additional studies with CIMS have been conducted with monodisperse OL, but analysis of the results involved insight from the mixed particle studies, so we will refrain from discussing these results until Sect. 4.4.3.1.

4.4.2.4 Reactive uptake: thermal desorption particle beam mass spectrometry

The TDPBMS method has also been applied to study the ozonolysis of submicron (~ 0.02 – $0.5 \mu\text{m}$ diameter) OL particles assuming Case 2 kinetics. Figure 6 shows a typical kinetic plot, with the slopes giving the value of $H(Dk_2)^{1/2}$. An uptake coefficient of $(1.3 \pm 0.2) \times 10^{-3}$ was calculated for pure OL particles. Interestingly, this study, which

11127

is the only one to date employing an environmental chamber, gave results similar to those with the CFT and AFT.

4.4.3 Reactive uptake by internally mixed particles and coatings

Organic particles in the troposphere are mixed particles (Alves et al., 2001; Duce et al., 1983; Guo et al., 2003; Hahn, 1980; Huang et al., 2005; Pio et al., 2001; Simoneit et al., 1988). Recently, a succession of papers has appeared in the literature reporting on the application of instrumental methods and models developed for the OL- O_3 HRS to examine the kinetics and/or products of ozonolysis of internally mixed particles (Hearn et al., 2005; Hearn and Smith, 2004b, 2005; Katrib et al., 2005a; Zahardis et al., 2006b; Ziemann, 2005) and multicomponent organic coatings (Knopf et al., 2005) that are more complex than this model system and more closely approximate real OA.

4.4.3.1 Reactive uptake of mixed particles: chemical ionization mass spectrometry

Hearn and Smith (2004b) have also measured the uptake coefficient of mixed particles of LA and OL with CIMS (Table 2). They found that the ratio of the uptake coefficients in the mixed particles of LA vs. OL is 1.37, which is slightly smaller than the theoretical value of 1.42 anticipated for doubling k_2 , and smaller than the ratio they measured for pure OL and LA particles (1.47) (Hearn and Smith, 2004b). As they note, this may indicate enhanced solubility and/or diffusion of O_3 in pure LA particles (Hearn and Smith, 2004b).

CIMS was applied to internally mixed, monodisperse particles of OL and MOL (Hearn et al., 2005). For 650 nm OL particles, the authors noted that all the cases that had exponential solutions for decay, namely Cases 1, 3 and 4, fit the data well. The authors eliminated Case 4 because the decay showed a dependence on the partial pressure of ozone, no dependency on the inverse square of the particle radius, and they assumed that OL diffusion was sufficiently fast to maintain a constant concentration throughout the particle. They eliminated Case 1 by noting that there is clearly a linear dependence

11128

of OL decay on the inverse of the particle radius. They concluded that the particle decay was given by Case 3, a surface reaction. This contradicts the prior studies, which indicated that this reaction was limited by ozone diffusion (Case 2) (Moise and Rudich, 2002; Morris et al., 2002; Smith et al., 2002). The authors calculated the uptake coefficient to be $(1.38 \pm 0.06) \times 10^{-3}$ for monodisperse OL from 600–1200 nm that had to be adjusted to account for secondary reactivity in the system as shall be described.

The uptake of ozone by MOL was investigated to try to evaluate the extent of secondary reactivity (Hearn et al., 2005) in the ozonolysis of OL, namely the formation of ACOAH by Cl via reaction with OL. Since this reaction proceeds through the addition of a Cl to the carboxyl group it would result in an additive loss to OL but would not deplete MOL. All loss of MOL would be via oxidative cleavage by ozone (Hearn et al., 2005). The best fit for 600–1100 nm MOL particles were given by Case 2 and γ was calculated to be $(1.23 \pm 0.10) \times 10^{-3}$. Although the values of γ were similar for pure OL and MOL, this does not explicitly imply that the uptake of the two particles is identical: “It is possible that O_3 solubility and/or diffusion are larger in the (MOL) particles than in (OL) particles and that this enhancement offsets an increased (OL) loss due to secondary reactions.” (Hearn et al., 2005)

The authors employed internally mixed particles of OL and MOL to investigate the extent of secondary reactions in the OL- O_3 HRS by eliminating possible differences in ozone solubility and diffusion. By changing the [MOL]/[OL] ratio, they were able to change the [Cl]/[OL] ratio, interrogating the extent of ACOAH formation. Figure 7 emphasizes the key results from these experiments. Without assuming a limiting case regime, the initial rates of reaction of OL and MOL for internally mixed particles are plotted as a function of the mole fraction of OL, χ . While the initial rate of reaction rose substantially for OL with decreasing χ , this was much less so with MOL. Figure 7 also presents the results of an analogous experiment using internally mixed particles of OL and *n*-hexadecane, the latter a saturated organic that is non-reactive towards ozonolysis, showing that the initial rate of decay of OL is approximately constant. This

11129

suggests that the increase in the initial rate of reaction of OL with decreasing χ was not simply due to a decrease in OL, but rather due to an increase in the [Cl]/[OL] ratio. Figure 8 is the appearance curve of a Cl rearrangement product, 9-methoxy-9-oxononanoic acid (MW = 202 u), a stable carboxylic acid resulting from ozonolysis of MOL. The yield of this species is significantly lower in the mixed particle compared to pure MOL because the Cl can react rapidly with OL. This effect is considerable; particles with a MOL:OL ratio of 3:1 show a reduction by a factor of 2 compared to the pure MOL particles.

Hearn et al. (2005) present further arguments that could account for the differences in the changes in the initial rate of reactions for OL and MOL with changing χ . One argument involves phase separation, where an OL shell forms around an MOL core. Subsequently, a faster reaction would occur with the MOL as opposed to OL; however, this morphology would cause a delay in the reaction time of MOL as a function of shell thickness which was not observed. One of the most significant results of this experiment (Hearn et al., 2005) is the estimate of the extent of reaction between the Cl and OL. The key assumption in this calculation is that the rates of reaction of OL and MOL are equal in the same particle (with other assumptions given by the authors). The authors suggested that the linearity shown in Fig. 7 is consistent with the reaction of the Cl with OL and they used the slope of the curve to calculate that 36% ($\pm 4\%$) of the OL lost is due to the reaction with the Cl. The authors also stated that “the linearity of this plot indicates that other secondary reactions involving (OL) and (MOL) must be negligible” (Hearn et al., 2005). The loss of OL to Cl was used as a correction for γ : the resulting *corrected* value of γ of $(8.8 \pm 0.5) \times 10^{-4}$ is in good agreement with the coated-wall studies (Moise and Rudich, 2002; Thornberry and Abbatt, 2004). It is also slightly lower than the value of the uptake coefficient of MOL, which the authors suggest is due to an enhanced solubility or diffusion of ozone in MOL compared to OL. They attribute this to the lower degree of order in MOL compared to OL. Under ambient conditions OL is an ordered liquid (Iwahashi et al., 2000, 1995, 1991) (Fig. 9), while MOL is probably an isotropic liquid under these conditions. Hearn et al. have

11130

proposed that this ordered liquid has a high density of carbon-carbon double bonds at the surface and therefore “reduces the rate of O₃ diffusion into the bulk and results in a surface-dominated reaction between O₃ and the double bonds of (OL).” Most or all of the ozonolysis occurs in the first monolayer of the ordered liquid OL by this model. In contrast, the low-ordered MOL has deeper diffusion of ozone and less surface reactions and follows Case 2 kinetics.

Key results and conclusions of the CIMS studies on mixed particles include

- Loss of CI to OL may be a significant loss route, with ACOAH the dominant products
- Secondary reactions of CI can consume OL and this should be accounted for in uptake calculations
- Accounting for these secondary reactions gives a value of γ similar to coated-wall reactor based measurements where ozone loss is measured directly. Other particle-based methods that do not account for secondary chemistry may have an artificially large value for γ

4.4.3.2 Reactive uptake of mixed particles: Aerodyne aerosol mass spectrometry

Katrib et al. (2005a) studied the uptake of ozone by internally mixed particles of OL and SA. An Aerodyne AMS was used to study nearly monodisperse 300 nm particles with OL concentration ranging from 0% to 100% relative to SA. SA is the saturated analogue to OL so it does not undergo *direct* oxidative processing by ozone. Figure 10 shows the decay profile of SA in particles with different OL:SA ratios as a function of ozone exposure. The authors proposed that the increase in SA decay with ozone exposure and OL concentration is due to the secondary chemistry facilitated by stabilized CI that are formed by ozonolysis of OL. They proposed that the CI reacts with the carboxylic acid of the SA forming ACOAH. They also noted that the decay profiles of SA and

11131

OL are very similar for 90/10 (OL: SA), 75/25 and 60/40 particles; however, with SA content greater than 50% the decay behavior of OL and SA differs.

The applicable limiting case for these mixed particles was not clear. It was noted that classification of the reactive uptake for a mixed particle that may contain some solid-phase (SA) of uncertain morphology was an even more complex issue than for the simpler system of pure OL, for which there exists still a high degree of uncertainty. The authors therefore opted for a data driven approach over the model driven approach (Katrib et al., 2005a) to determine the reactive uptake. The data-driven approach applies the steady-state assumption to the concentration of dissolved ozone in the particle, such that further ozone uptake is driven by chemical reaction and it is assumed that monitoring the loss of volume-averaged ozone is equal to measuring the rate of reaction of OL. The authors acknowledge that the second assumption has inherent inaccuracies since some of the OL is consumed by CI generated in ozonolysis.

The authors applied this method to non-spherical particles, such as those with SA (which was inferred from microscopy), then further adapted the expression for γ for the Aerodyne AMS method that measures the mass of an aerosol population. This approach yielded:

$$\gamma = \frac{-dm_{OL}/dt}{(P_{O_3} \bar{c}/4RT)(MW_{OL} NA)} \quad (11)$$

Here m_{OL} is the aerosol mass of OL, N is the number concentration of particles, and A is the particle surface area. Because [OL] and γ both decrease over time, the authors extrapolated their decay data to zero time and calculated an initial uptake coefficient, γ_o . The pressure of ozone was varied at a fixed exposure time and dm_{OL}/dt was approximated as $\Delta m_{OL}/(\Delta t)$, with A calculated for a known diameter particle, giving an upper-limit estimate of γ_o by Eq. (11). This process was repeated for other ozone pressures, with further considerations given by the authors, and then averaged, giving γ_o for a given OL/SA composition. This method gave $(1.25 \pm 0.2) \times 10^{-3}$ for pure OL, which is in good agreement with the prior Aerodyne AMS study (Katrib et al., 2004)

11132

that was model driven.

The authors consider the uptake coefficient reported as the upper limit, since there was no accounting for the loss of OL to secondary reactions with Cl. If a correction in accord to Hearn et al. (2005) is made, the value of γ ($\sim 8 \times 10^{-4}$) is in good agreement with that of Hearn et al. (2005) ($\sim 9 \times 10^{-4}$). Katrib et al. (2005a) found that the upper-limit value of γ_o decreased linearly from OL/SA 100/0 to 60/40, from $(1.25 \pm 0.2) \times 10^{-3}$ to $(0.60 \pm 0.15) \times 10^{-3}$; however, at OL/SA 50/50 the authors noted an abrupt drop in the upper-limit value of γ_o to $(0.15 \pm 0.1) \times 10^{-3}$ which remained approximately constant toward higher particle content of SA. Similar decreases have been observed by Knopf et al. (2005) for alkanolic acid/oleic acid mixtures, as shall be discussed in Sect. 4.4.3.4

Katrib et al. (2005a) compared the results of the parameters of their Aerodyne AMS experiments: unreacted OL and SA at high ozone exposure, the initial uptake coefficient, and particle beam width and discerned there were three distinct composition regions that have different effects on these parameters (Fig. 11). In the first region, the linear increase in SA corresponds with a linear trend in the parameters. In region 2 there is an abrupt change in all the parameters, though the change appears monotonic. In the third composition region, there are no changes in the parameters or the change is minimal with increasing SA content

The authors suggest three postulates to explain the trends in the parameters, all of which relate to morphological changes in the particles:

- Supersaturation
- SA binding OL as an impurity in its crystal lattice
- Formation of semi-permeable gels of SA that contain some liquid OL

The authors noted (Katrib et al., 2005a), in regards to OL: “For all compositions having SA content greater than 90/10, the reaction kinetics appear to have a two-step behavior, showing an initial fast decay for low ozone exposure followed by an apparent absence of further reaction at high ozone exposure.” Similar kinetic effects have been

11133

observed in other mixed particle studies (Hearn and Smith, 2005; Ziemann, 2005), as noted by the authors.

In summary:

- A data driven approach was used to determine $\gamma \sim 1 \times 10^{-3}$ for OL, similar to other particle-based methods that do not correct for secondary chemistry
- Secondary chemistry via Cl was indicated including reactions with a saturated FA (SA) that is not susceptible to direct ozonolysis
- Nonlinearity in γ and other parameters may arise from morphological changes in the particle

4.4.3.3 Reactive uptake of mixed particles: thermal desorption particle beam mass spectrometry

Ziemann applied TDPBMS to mixed particles (Ziemann, 2005) employing an environmental chamber. The internally mixed particles included 10/90 (OL) mixtures with non-volatile components: DOS, C17 and C16. None of these species are susceptible to oxidative cleavage by ozone, allowing for assessment of how liquids and solids affect reactive uptake.

Figure 6 shows the decay profiles of pure OL and the three internally mixed particles. Case 2 of the resistor model was applied, assuming a thin diffuso-reactive layer relative to the particle diameter. The kinetics of pure OL and DOS/OL are seen to be very similar, reacting essentially completely with ozone within 2–3 min. It was noted by the author that the reaction of the mixtures containing the alkanolic acids, C16 and C17, are “initially almost as fast (as pure OL), but then slow down dramatically within ~ 2 min such that $\sim 65\%$ and $\sim 80\%$ of the OL has reacted after ~ 8 min.” These effects are attributed to the phase equilibria. In the particles with C16 and C17, the fast and slow regimes may be due to the particles having two phases, one that is pure liquid OL, the

11134

other being a semi-solid mixture of OL and the alkanolic acid and diffusion impeded in these regions leading to a slower reaction rate (Knopf et al., 2005).

Using the results of Case 2, Ziemann (2005) calculated uptake coefficients for OL/DOS, OL/C16 and OL/C17 at $(1.1\pm 0.4)\times 10^{-3}$, $(0.13\pm 0.1)\times 10^{-3}$ and $(0.25\pm 0.2)\times 10^{-3}$ (Ziemann, 2005). Notice that the OL/DOS uptake coefficient is very similar to that of pure OL, $(1.3\pm 0.2)\times 10^{-3}$. Conversely, for the mixed particles with alkanolic acids, the values are about one order of magnitude lower than the uptake coefficient of pure OL, which is attributed to the trapping of OL. This is quite different from the value of γ_o determined by Katrib et al. (2005a) for the corresponding composition of OL/SA; the OL/SA particles with 90% OL had an estimated γ_o of $\sim 1\times 10^{-3}$. However, the mixed particles of OL and C16 or C17 are very similar to the value of γ_o for OL/SA particles with 50% or less OL content, $(0.15\pm 0.10)\times 10^{-3}$.

In summary:

- γ decreases by about one order of magnitude (to $\sim 10^{-4}$) in mixed particles that may have semisolid phases

4.4.3.4 Reactive uptake of mixed coatings

Knopf et al. (2005) have applied a rotating-wall flow tube reactor to study the ozonolysis of lauric acid/OL (C12/OL) and myristic acid/OL (C14/OL) mixtures. Also investigated by this method were multicomponent mixtures that were proxies to meat-cooking aerosols similar to those observed in field studies (Hildemann et al., 1994; Rogge et al., 1991; Schauer et al., 1999). A key difference in this methodology as compared to the AFT experiments is that in the former less than 3% of the film is oxidized, as compared to the aerosol based experiments where most or all of the particle is often subjected to longer exposures. Further, Knopf et al. (2005) used atmospherically relevant ozone concentrations (on the order of 10^{12} molecules cm^{-3} ; Fenger, 1999), which are several orders of magnitude lower than those used in most of the AFT experiments.

The authors varied the C12 and C14 concentrations relative to OL such that they

11135

had completely liquid mixtures as well as solid-liquid mixtures that, in the latter case, had liquid OL and the alkanolic acid as a solid. Additionally, films were prepared by two different methods to investigate the effects of preparation on uptake of ozone. The "slow cooling method" involved melting a solid-liquid mixture and crystallizing it on the wall of the tube and slowly cooling, while in the "fast cooling method," a preheated tube was rapidly immersed in liquid N_2 to prepare a solid film. It should be noted that the films appear as wax-like solids with different overt morphology, but, as the authors note, although solids in appearance, the films must contain liquid by the lever rule.

By monitoring ozone loss, γ of liquid OL (at $T\sim 286\text{--}298\text{ K}$) and solid OL (at $T\sim 278\text{--}285\text{ K}$) were determined to be $(7.9\pm 0.3)\times 10^{-4}$ and $(0.64\pm 0.05)\times 10^{-4}$, respectively (Knopf et al., 2005). As shown in Table 2, these values are in good agreement with other studies employing CFT (Moise and Rudich, 2002; Thornberry and Abbatt, 2004), and somewhat smaller than γ measured in most aerosol based studies that do not employ corrections accounting for secondary chemistry (Katrib et al., 2005a; Morris et al., 2002; Smith et al., 2002; Ziemann, 2005). As in the case of the coated-wall studies by Moise and Rudich (2002), the solid-phase OL coatings have an uptake approximately one order of magnitude smaller than the liquid. Unlike the uptake of pure solid and liquid OL, the uptake of C12/OL and C14/OL are not continuous functions (Knopf et al., 2005) of the mixture ratio. As the authors note: "When a small amount of (C12) or (C14) is added to (OL), there appears to be a step change in the uptake coefficient, after which the uptake follows a continuous function."

The values of γ for the liquid and solid-liquid binary mixtures are given in Table 2. Notice that the value of γ for the C12/OL and C14/OL liquid mixtures is very similar, ranging from $(4\text{--}7.2)\times 10^{-4}$, decreasing with increasing concentration of the alkanolic acid and of similar order of magnitude of pure liquid OL. The uptake coefficient for the mixed phase coatings decreases by up to an order of magnitude, compared to the liquid mixtures. As noted by Knopf et al. (2005) this decrease in γ probably originates from "the solid (forming) an interconnected network by dendritic growth, aggregation of crystals, or eutectic solidification, which can result in lamellar or rod microstructures."

11136

These structures slow the diffusion of ozone and OL, trap OL, and/or have other effects that cause the uptake of ozone to be smaller than the liquid-phase. The slow-cooled solid-liquid mixtures generally had a smaller value of γ than the corresponding fast-cooled mixtures (Knopf et al., 2005) with the authors proposing that the slow cooling structure trapped more OL than the fast cooling one.

OA in the troposphere are far more complex than proxies investigated to date in the laboratory. In this regard, films with compositions resembling meat-cooking aerosols (Rogge et al., 1991; Schauer et al., 1999) have been prepared (Knopf et al., 2005) and subjected to ozonolysis. Mixed particles with 5, 9, and 15 components were prepared, with OL as the major component in all cases, followed in order of mass by other FA, then by the other classes of organics i.e. dicarboxylic acids, alkanes, alkanones, and amides. These mixtures may represent the most realistic organic mixture found in aerosol particles with respect to identified mass. The phase behavior of these complex mixtures is not well-known, but the authors evoked thermodynamic arguments to speculate that OL should remain in the liquid state, while the alkanolic acids may be solids (Knopf et al., 2005). The value of γ ranged from $(1.6\text{--}6.9)\times 10^{-5}$ for these mixtures, less than their γ for liquid OL by at least one order of magnitude, with the upper-limit similar to solid OL with the slower-cooled films having smaller values of γ . The differences in γ of the slow- and fast-cooling systems probably stem from the trapping of OL and morphological differences in the coatings as a function of preparative procedure.

In summary:

- Morphological differences can lead to significant changes in γ which, compared to pure OL, decrease by about one order of magnitude when a medium is frozen or is a complex mixture

4.5 Supercooling in mixed particles

Hearn and Smith have described the uptake of ozone by OL/C14 with CIMS (Hearn and Smith, 2005), revealing that mixed particles can exist in a supercooled, non-equilibrium

11137

state. At room temperature, the rate of decay of OL to completion in OL/C14 mixtures was approximately the same as for pure OL, indicating a supercooled mixture. This was not the expected result since C14 is a solid at room temperature and should slow the rate of decay (Knopf et al., 2005). The authors estimated that mixtures with the most C14 enrichment had the largest supercooling (32°C) at room temperature. This estimate was based on the assumption that the complete loss of OL in the ozonized particles corresponded with completely liquid particles, giving the lower limit of supercooling for the C14/OL particles. As noted by the authors, the presence of supercooled OA in the troposphere and the implications on ozone loss is an unexplored area.

5 Discussion

The OL-O₃ HRS continues to serve as a proxy to aid in elucidating themes of processing of HRS consisting of condensed-phase organics by gas-phase trace oxidants. The following sections discuss the atmospheric implications of oxidative processing, especially by ozone, of OA, based upon what has been learned from this and related proxies. These implications regard atmospheric lifetime, CCN ability of OA, and subsequently the effects on radiative forcing, and the oxidative capacity of the troposphere.

5.1 Lifetime of unsaturated organic particulate in the troposphere

There is clearly an enhancement in the reaction rate between ozone and alkenes, such as OL, when the organic is in the form of particulate or a coating as compared to the gas-phase (Hearn and Smith, 2004b; Moise and Rudich, 2001; Morris et al., 2002; Thornberry and Abbatt, 2004; Wadia et al., 2000). For example, the uptake coefficient of pure liquid OL is on the order of 10^{-3} (Hearn and Smith, 2004b; Katrib et al., 2005a; Knopf et al., 2005; Moise and Rudich, 2002; Morris et al., 2002; Smith et al., 2002; Thornberry and Abbatt, 2004; Ziemann, 2005), which corresponds to approximately one reaction (oxidative cleavage of OL) per 1000 collisions. For comparison, analo-

11138

gous homogeneous gas-phase reactions have rate constants on the order of 10^{-15} – 10^{-17} $\text{cm}^3 \text{ molecule}^{-1} \text{ s}^{-1}$ (Atkinson, 1997; Atkinson et al., 1997; Finlayson-Pitts and Pitts Jr., 1999), which corresponds to approximately one reaction per 10^5 – 10^7 collisions (Hearn and Smith, 2004b).

5 There is an anomaly in the atmospheric half-life (and lifetime) of OL, regarding loss to ozone, between laboratory based kinetic measurements and field measurements. This was noted by Morris et al. (2002) who used their experimental value of $H(Dk_2)^{1/2}$ to estimate an atmospheric half-life on the order of minutes for submicron OL with 100 ppb O_3 , while field measurements suggested lifetimes on the order of days (Rogge
10 et al., 1991). Experimentally based calculations by Smith et al support the estimate by Morris and coworkers; at $[\text{O}_3]=100$ ppb, a 50 nm particle of OL would take less than two minutes for 99% of the OL to react (Smith et al., 2002). Similarly, Hearn and Smith (2004b) estimated that for the same concentration of ozone, particulate OL would have a lifetime of a few minutes.

15 This anomaly in OL half-life between laboratory and field studies probably arises from the OL in the latter case being part of a multicomponent viscous, semi-solid particle (Morris et al., 2002). For example, in the urban environment, meat-cooking aerosols contain not only OL but SA and palmitic acid as well as many other components (Schauer et al., 1999). Smith et al. (2002), using an organic aerosol density
20 of 1.5×10^5 particles cm^{-3} typical of an urban setting (Heintzenberg, 1989), estimated that for particles with radii of 25 nm and an average OL content of 1%, the OL lifetime with respect to ozonolysis is 36 hrs. This is also demonstrated by Ziemann (2005), who calculated OL lifetimes of ~ 15 min for pure OL particles vs. 15 h for OL in mixed particles with alkanolic acids.

25 The diffusion of OL would most likely be impeded in a viscous multicomponent particle, such as meat-cooking aerosol, which would increase the OL lifetime compared to that of pure OL particulate. Moreover, in multicomponent particles with liquid and solid-phases, OL could be trapped in the solid-phase (Katrib et al., 2005a). For example, this was demonstrated in SA-OL mixed particles: OL in liquid regions reacts quickly,

11139

while OL trapped in the solid SA is “essentially unavailable for reaction” (Katrib et al., 2005a). Katrib and coworkers (Katrib et al., 2005a) noted this second effect may impact quantitative source apportionment, where OL is used to apportion the contribution of meat-cooking to urban particulate. The OL in the solid fraction would be detected and
5 used in quantitative source apportionment, with the amount of OL in the liquid portion diminished due to ozonolysis; hence, meat-cooking would suffer from a negative bias in quantitative source apportionment assessment (Katrib et al., 2005a).

The coated wall studies of proxies of meat-cooking aerosols by Knopf et al. (2005) at this time may best elucidate the differences in the lifetime of pure OL as opposed
10 to OL as part of a multicomponent organic admixture. While their studies indicate that the lifetime of OL is not significantly affected by the addition of a second component, such as an alkanolic acid if there is no corresponding change in phase, the presence of a solid-phase can cause the lifetime of OL to increase by more than an order of magnitude. They estimated that the lifetime of OL in their 15 component proxy to meat-cooking aerosol was ~ 75 min as opposed to simpler proxies (OL/C12 or C14) that had
15 lifetimes ~ 3.5 – 5 min for the liquid solutions (Knopf et al., 2005).

The physical state of the FA in the condensed-phase medium has a significant impact on the uptake of ozone. Moise and Rudich (2002) showed the uptake of ozone by OL and LA decreased by approximately an order of magnitude upon freezing. Changes in
20 temperature without a corresponding change in phase probably have less of an impact on reactive uptake, as shown for the case of OL, LA, and LN, which all have a small positive temperature dependency as liquids (Thornberry and Abbatt, 2004).

Uptake has also been shown to be affected by the microstructure of the organic medium (Knopf et al., 2005). With multicomponent coatings, slow cooled solid-liquid
25 mixtures generally had a smaller uptake coefficient than fast cooled mixtures with similar composition. This was attributed to the microstructure of the solid (Knopf et al., 2005), with the film produced by slow cooling having a microstructure that either more effectively traps OL or reduces diffusion compared to its congener prepared by fast cooling. Moreover, aging of the semi-solid films affects the uptake of ozone, with older

11140

films having an increased γ , and a maximum value at ~ 10 h. The authors attributed this effect to either the relaxation of a non-equilibrium phase to a stable phase, or to Ostwald's ripening (Chou and Hong, 2004).

As noted earlier, Hearn and Smith (2005) demonstrated for the first time that mixed organic particles (OL/C14) can exist as supercooled droplets. OL in a 200 nm solid-liquid particle exposed to 100 ppb O_3 would have a lifetime of 60 min from the noted reaction of solid OL/C14; however in the supercooled droplet this lifetime would be only ~ 5 min. The different reactive uptake by supercooled OA may have atmospheric implications, particularly for the urban environment. In the experiments by Hearn and Smith (Hearn and Smith, 2005), organic particulate was generated by homogeneous nucleation of heated vapors, at a similar temperature of real meat-cooking aerosols (Rogge et al., 1991) suggesting these aerosols might be supercooled. To our knowledge, there have been no field studies to confirm the presence of supercooled mixed OA in the troposphere. The observation of the longer lifetime of OL in urban particulate (Rogge et al., 1991) than that of OL in laboratory measurements, would appear to indicate that supercooling of OA does not persist under atmospheric conditions; however, the OL may react quickly with ozone, increasing γ , while the particle is supercooled prior to achieving equilibrium and having a solid-phase form (Hearn and Smith, 2005).

Little is known about the thermodynamics of real atmospheric organic particulate and these experimental observations from HRS featuring relatively simple OA and coatings elucidate many of the challenges faced by researchers needed to understand the processing of organic particulate in the troposphere. Factors including aging, temperature, and motif of particulate formation, composition, and phase equilibrium all appear to affect the uptake and need further, more progressive consideration.

5.2 Oxidatively processed organics as cloud condensation nuclei

Ozonolysis results in an oxygen enriched OA containing hydrophilic species including acids, diacids, and a variety of peroxides, including HMW polymers that are formed by secondary reactions. Oxygen enrichment has been demonstrated to be concomitant

11141

with an increase of particle density. This effect is significant, with density increasing from 0.89 g cm^{-3} to 1.12 g cm^{-3} and continuing to increase along with oxygen enrichment with prolonged exposure, even after all the OL has reacted (Katrib et al., 2005b). This is most likely due to secondary chemistry in the system. Oxygen enrichment generally corresponds to greater hygroscopicity (Asad et al., 2004; Broekhuizen et al., 2004; Hung et al., 2005) and the presence of more water soluble components and is a good indicator of CCN activation (Cruz and Pandis, 1997; Moise and Rudich, 2000; Novakov and Corrigan, 1996). The enhanced hygroscopicity afforded by ozonolysis of OL was shown by Asad et al. (2004) in the four-fold increase in the water-sorbing capacity of a highly processed film compared to an unprocessed one. Hung et al. (2005) also showed that the critical RH at which OL droplets took on water was reduced from over 99% to 91% after exposure to ozone, which is indicative of increased hygroscopicity.

Another consequence of increased oxygen enrichment of OA by ozonolysis is a decreased contact angle with water (Moise and Rudich, 2000, 2001), again leading to an enhancement of the CCN ability (Raymond and Pandis, 2002). Activation depends on the solubility of the species and the ability to spread water or form a finite contact angle (Raymond and Pandis, 2002). Typical FA have relatively large activation diameters as predicted from Köhler theory (Köhler, 1936); for example, palmitic acid and SA have experimental activation diameters of over 200 nm at supersaturations of 0.3 and 1% (Raymond and Pandis, 2002) and OL has been shown not to activate (0.6% supersaturation) with a dry diameter up to 140 nm (Kumar et al., 2003). In short, the low solubility of water in HMW FA renders them particularly poor CCN; however, studies on submicron OL and LA particles, employing a tandem differential mobility analyzer coupled to a flow reactor, showed that high exposure to ozone (0.42 atm s) had an effect on the CCN activity of OL and the critical activation diameter (Broekhuizen et al., 2004). At low ozone exposures ($< 1 \times 10^{-4} \text{ atm s}$), there was a loss of about 25% of the original particle volume for OL, due to volatilization of nonanal; however, there was no increased CCN activity. However, at the higher ozone exposure, pure OL became CCN active with a critical activation diameter of 161 nm at 0.6% supersaturation.

11142

This appeared to be a direct effect of the oxidation of OL, since its saturated congener, SA, showed no activation at 0.6% supersaturation with an ozone exposure of 0.5 atm s and particle sizes up to 300 nm. It should be noted that the doubly unsaturated LA never became activated even at high exposures. The inability of the unsaturated LA to activate is not as clear cut as for the saturated SA and the authors suggested that this might be due to the reactivity of the CI with the double bonds of LA, with a faster rate of polymer formation (than OL) and these products being more highly branched and complex (Broekhuizen et al., 2004). Clearly, the nuances of the oxidative processing of specific FA and the implications to the troposphere, including the ability to act as CCN, need further investigation.

Mixed particulate shows a markedly different behavior than pure FA aerosol in terms of activation (Broekhuizen et al., 2004). As shown in Fig. 12, mixed OL/methanol particles became activated by ozone under atmospherically relevant exposures. This is an important result in that not only are organic particles in the troposphere composed of many components (Alves et al., 2001; Duce et al., 1983; Guo et al., 2003; Hahn, 1980; Huang et al., 2005; Pio et al., 2001; Simoneit et al., 1988) but alcohols are commonly observed in biogenic particulate (Alves et al., 2001; Pio et al., 2001; Rogge et al., 1993; Simoneit et al., 1988; Simoneit et al., 1991; Simoneit and Mazurek, 1982).

More detailed studies need to be engaged similar to that of Broekhuizen and coworkers (Broekhuizen et al., 2004) that look at the role of oxidative processing on activation of more realistically formulated multicomponent organic particulates that are better proxies for actual aerosols of the troposphere.

5.3 Radiative forcing by oxidatively processed organic particulate

There are broad implications of oxidatively processed OA on forcing mechanisms that affect the energy budget of the Earth-atmosphere system. Some of these implications stem from the enhancement of the processed OA to act as CCN. As summarized in a recent review (Lohmann and Feichter, 2005), aerosols affect the global climate by scattering both solar and thermal radiation, as well as acting as CCN and ice nuclei.

11143

The first two mechanisms are considered direct forcing effects (Haywood and Boucher, 2000), while the formation of CCN and ice nuclei are considered indirect aerosol effects (Haywood and Boucher, 2000; Lohmann and Feichter, 2005) and are perhaps the greatest source of uncertainty in understanding radiative forcing in the atmosphere (McFiggans et al., 2006). Oxidative processing of OA forms more hygroscopic particulate and may promote the Twomey effect by an increase in small droplets in clouds. The Twomey effect is a negative forcing due to scattering of solar radiation by smaller droplets in clouds with constant water content (Lohmann and Feichter, 2005; Twomey, 1959).

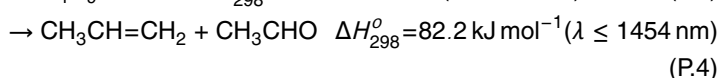
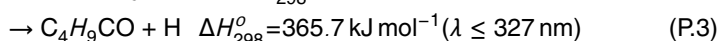
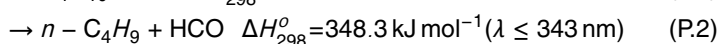
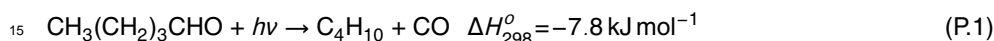
We suggest that the formation of photoreactive aldehydes by ozonolysis of OA containing unsaturated species could contribute to a positive forcing. Absorption of solar radiation by these species could enhance local heating and promote evaporation of cloud droplets (i.e. the semi-direct effect) (Lohmann and Feichter, 2005), decreasing cloud cover and the liquid-water path, leading to positive forcing (Johnson et al., 2004; Lohmann and Feichter, 2005). This is in contrast to the negative forcing of cloud albedo usually associated with OA. We suggest further that consideration should be given not only to the formation of volatile carbonyl containing compounds, like nonanal, but also to less volatile carbonyl containing compounds that are retained, at least in part, in the particulate, such as 9-oxononanoic acid and polymeric species that have been detected in many of the studies of the OL-O₃ HRS mentioned in this review.

The role that oxidative processing of OA has in contributing to the radiative forcing is a complicated problem and still in the early stages of description. To fully describe radiation budgeting in the Earth-atmosphere system we have to develop a better description of the contribution of OA to cloud albedo, CCN mediated indirect effects from OA, and possibly semi-direct effects. Understanding these roles is imperative in light of current uncertainties in our predictions of global warming trends and climate sensitivity, which depend in part on radiation budgeting by OA.

11144

5.4 Oxidatively processed OA and the oxidative capacity of the troposphere

Ozonolysis of unsaturated FA may have implications towards the oxidizing capacity of the troposphere. Ozonolysis of OL and other unsaturated FA results in the formation of long chain, volatile aldehydes that are likely released to the troposphere. Aldehydes are photoreactive species that can undergo photolysis to alkyl radicals with most studies to date focusing on lower MW products (Finlayson-Pitts and Pitts Jr., 1999; Graedel et al., 1976; Grosjean, 1982), although there have been some experimental photochemical studies on moderate MW aldehydes, such as pentanal (Cronin and Zhu, 1998). Aliphatic aldehydes have a weak absorption band from approximately 240–360 nm (Cronin and Zhu, 1998) and HCO is a common product of their photolysis (Finlayson-Pitts and Pitts Jr., 1999). Typically, the photolysis of larger aldehydes is more complex than smaller aldehydes like formaldehyde and acetaldehyde. For example, the following pathways of photolysis of *n*-pentanal have been proposed (Cronin and Zhu, 1998):



Alkyl radicals, such as those formed in pathway (P.2), lead to the formation organic peroxy radicals, RO₂, which is the most significant reaction pathway to the alkyl radical under tropospheric conditions (Aumont et al., 2005). The peroxy radical, which can go on to react with NO, NO₂, NO₃, HO₂, RO₂ (Aumont et al., 2005) and other species, plays many important roles central to tropospheric chemistry, such as in the dynamics of NO_x affecting the conversion of NO to NO₂ (Atkinson, 1998). Both CHO and the peroxy radical are involved in regulation of the hydroperoxyl radical, HO₂. For example,

11145

CHO can react with molecular oxygen forming HO₂ and CO (Graedel et al., 1976). The RO₂ that is formed from the alkyl radical can react with HO₂ forming ROOH (Atkinson, 1998) or can be converted to RO (for example by reactions with NO) that can react further with molecular oxygen forming an aldehyde and HO₂ (Graedel et al., 1976). The hydroperoxyl radical can form an adduct with certain aldehydes as well (Evleth et al., 1993; Finlayson-Pitts and Pitts Jr., 1999), but despite this being a fast reaction, the decomposition back to aldehyde is fast as well so this reaction does not appear to be a significant sink of aldehydes (Finlayson-Pitts and Pitts Jr., 1999). Figure 13 illustrates some of the key features of gas-phase aldehydes and their photolysis products that may affect the oxidative state of the troposphere.

Gas-phase aldehydes are involved in a host of other diverse reactions. Oxidants including OH, NO₃ and Cl can abstract the aldehydic hydrogen, forming the reactive RCO radical (Finlayson-Pitts and Pitts Jr., 1999) that can be further oxidized by molecular oxygen. Many of the products of these reactions are involved in the formation of O₃ and peroxyacetyl nitrate. Recent box model studies suggest that aldehydes, such as acetaldehyde, may be important in the halogen cycle at the marine boundary layer by promoting the conversion of Br to HBR and other species (Toyota et al., 2004).

Most of the field-based measurements of carbonyls have focused on studying lighter aldehydes (Finlayson-Pitts and Pitts Jr., 1999; Grosjean, 1982; Moussa et al., 2006) such as formaldehyde and acetaldehyde. The detection of higher carbonyls in the field is in its nascent stage and there are many questions about the actual sources of these aldehydes and other higher carbonyls in general (Hellén et al., 2004).

Clearly, the impact of the ozonolysis of unsaturated FA aerosol and the subsequent emission of volatile aldehydes into the environment on the oxidative capacity of the troposphere merits further investigation.

11146

6 Conclusions

The OL-O₃ HRS is a proxy system that has been used to improve our understanding of the oxidative processing of OA that occurs in the troposphere. More complex multicomponent systems are being investigated, but these aerosols and films are in most cases still far simpler than real OA. In this paper we have tried to present a key theme emerging from these experiments – heterogeneous processing by ozone, even with simple proxies, is complicated by secondary chemistry, phase equilibria and other thermodynamic effects such that to accurately access the details of reactive uptake and product formation presents a formidable task.

10 *What have we learned and what are the implications?*

- In most studies, the measured uptake coefficient of ozone by OL is $\sim(0.7-1 \times 10^{-3})$, with the smaller value probably being more accurate for atmospheric OA:
 - a) Direct measure of ozone loss by CFT tends towards the lower limit
 - b) Methods that correct for secondary chemistry tend towards the lower limit
- 15 – **Implication:** The uptake of ozone by particle-phase unsaturates is probably more significant per unit mass than corresponding gas-phase organics, being enhanced by 2–4 orders of magnitude. Tropospheric OA may be a significant sink of ozone.
- The uptake coefficient may decrease significantly (~ 1 order of magnitude) in mixed-particles and coatings, especially when a solid or semisolid phase is present
- 20 – **Implication:** OL lifetime in the troposphere may be extended by the morphology of real OA and could bias quantitative source appointment
- The formation of peroxides through the secondary reactions of Cl appears to be significant, and high yields are possible

11147

- A diversity of products including SO and peroxidic polymers are formed
- These products are generally HMW, low volatility, and hydrophilic
- **Implication:** The formation of these products may correspond with increases in CCN ability, including lowering the activation radius of the particle. Tropospheric OA may contain protic species, such as water, that may promote the formation of peroxides, enhancing these effects further.
- 5 – **Implication:** Ozonolysis of OA may enhance the negative forcing associated with indirect aerosol effects that are largely mediated by CCN
- Volatile aldehydes are formed from the ozonolysis of FA, with nonanal being one of the major products in the OL-O₃ HRS
- 10 – **Implication:** Ozonolysis of OA may produce products that contribute to the oxidative capacity of the troposphere
- **Implication:** Aldehydes are photochemically active in the near-uv and semi-direct radiative effects with corresponding positive forcing are inferred

15 *What are some important questions and topics that must be addressed?*

- We need to establish whether the resistor model represents an accurate physical description of the heterogeneous microphysical processing or if it is just a convenient method to fit data. Although this model gives values for γ that are reasonably close to those determined by coated-wall tubes, there are some problems:
 - 20 a) There is a linear dependence of γ on the particulate radius in some experiments but this is not observed in other experiments (cf. Hearn et al., 2005; Smith et al., 2002)
 - b) There is no direct accounting for secondary chemistry by the model

11148

- We need to perform multiple quantitative assessments of the total peroxides yielded by ozonolysis of OL and other unsaturated organics, especially in multicomponent proxies
- 5 – We need to accurately describe the types of peroxides formed and under what conditions they are formed. We need to understand how peroxide yields and the types formed vary with the addition of ubiquitous protic species that may affect total peroxide yield and the types of product formed.
- We need to accurately measure the lifetime of these peroxides in oxidatively processed aerosol
- 10 – Proxies that specifically model atmospheric aerosol types need to be developed. This includes proxies for both biogenic and anthropogenic emissions.
- A better thermodynamic description of multicomponent OA is needed to understand the potential roles of phase equilibria, supercooling and other effects that may affect reactive uptake and chemical kinetics, lifetime of specific analytes, and other processes
- 15 – We need to look at the effects of more complicated (realistic) processing by multiple gas-phase species, including systems with multiple oxidants

11149

Appendix A: List of abbreviations

ACOH	α -Acyloxyalkyl Hydroperoxide(s)
AFT	Aerosol flow tube(s)
ALOH	α -Alkyloxyalkyl Hydroperoxide(s)
AMS	Aerosol Mass Spectrometer (Spectrometry)
ATR-IR	Attenuated Total Internal Reflectance Infrared Spectroscopy
CCN	Cloud Condensation Nuclei
CFT	Coated flow tube(s)
CI	Criegee Intermediate(s)
CIMS	Chemical Ionization Mass Spectrometry (Spectrometer)
C12	Lauric Acid
C14	Myristic Acid
C16	Hexadecanoic Acid
C17	Heptadecanoic Acid
DOS	Dioctyl Sebacate
E-O ₃ RS	Ethene-Ozone Homogenous Reaction System
FA	Fatty Acid(s)
FT-IR	Fourier Transform Infrared Spectroscopy (Spectrometer)
GC	Gas Chromatography
HMW	High Molecular Weight
HRS	Heterogeneous Reaction System(s)
IGAC	International Global Atmospheric Chemistry Project
IGBP	International Geosphere Biosphere Programme
iLEAPS	Integrated Land Ecosystem Process Study
IR	Infrared
LA	Linoleic Acid
LC-MS	Liquid Chromatography Mass Spectrometry
LN	Linolenic Acid

11150

MOL	Methyl Oleate
MS	Mass Spectrometer (Spectrometry)
MW	Molecular Weight
OA	Organic Aerosol
OL	Oleic Acid
OL-O ₃ HRS	Oleic Acid-Ozone Heterogeneous Reaction System
OOA	9-Oxo-octadecanoic Acid
PERCI-AMS	Photoelectron Resonance Capture Ionization Aerosol Mass Spectrometry
PO	Primary Ozonide
RH	Relative Humidity
SA	Stearic Acid
SMPS	Scanning Mobility Particle Sizer
SO	Secondary Ozonide(s)
SOA	Secondary Organic Aerosol
SOLAS	Surface Ocean-Lower Atmosphere Study
TDPBMS	Thermal Desorption Particle Beam Mass Spectrometry
T-O ₃ S	1-Tetradecene-O ₃ System
TOF	Time-of-Flight
TPTD	Temperature Programmed Thermal Desorption

Acknowledgements. The authors gratefully acknowledge the financial support of the National Science Foundation (ATM-0440074).

References

- 5 Abbatt, J. P. D. and Nowak, J. B.: Heterogeneous interactions of HBr and HOCl with cold sulfuric acid solutions: Implications for Arctic boundary layer bromine chemistry, *J. Phys. Chem. A*, 101, 2131–2137, 1997.

11151

- Alves, C., Pio, C., and Duarte, A.: Composition of extractable organic matter of air particles from rural and urban Portuguese areas, *Atmos. Environ.*, 35, 5485–5496, 2001.
- Asad, A., Mmereki, B. T., and Donaldson, D. J.: Enhanced uptake of water by oxidatively processed oleic acid, *Atmos. Chem. Phys.*, 4, 2083–2089, 2004.
- 5 Ashbaugh, L. L., Carvacho, O. F., Brown, M. S., Chow, J. C., Watson, J. G., and Magliano, K. C.: Soil sample collection and analysis for the Fugitive Dust Characterization Study, *Atmos. Environ.*, 37, 1163–1173, 2003.
- Atkinson, R.: Gas-phase tropospheric chemistry of volatile organic compounds: 1. Alkanes and alkenes, *J. Phys. Chem. Ref. Data*, 26, 215–290, 1997.
- 10 Atkinson, R.: Gas-phase degradation of organic compounds in the troposphere, *Pure and Appl. Chem.*, 70, 1327–1334, 1998.
- Atkinson, R., Baulch, D. L., Cox, R. A., Hampson Jr., R. F., Kerr, J. A., Rossi, M. J., and Troe, J.: Evaluated kinetic, photochemical, and heterogeneous data for atmospheric chemistry. 5. IUPAC subcommittee on gas kinetic data evaluation for atmospheric chemistry, *J. Phys. Chem. Ref. Data*, 26, 521–1011, 1997.
- 15 Aumont, B., Szopa, S., and Madronich, S.: Modelling the evolution of organic carbon during its gas-phase tropospheric oxidation: development of an explicit model based on a self-generating approach, *Atmos. Chem. Phys.*, 5, 2497–2517, 2005.
- Bailey, P. S.: *Ozonation in Organic Chemistry*, Academic Press, New York, 1978.
- 20 Bailey, P. S. and Ferrell, T. M.: Mechanism of Ozonolysis. A more flexible stereochemical concept, *J. Am. Chem. Soc.*, 100, 899–905, 1978.
- Bailey, P. S., Ward, J. W., Potts III, F. E., Chang, Y.-G., and Hornish, R. E.: Ozonation of hindered vinyl alcohols. Production of free radicals by ozonation, *J. Am. Chem. Soc.*, 96, 7228–7232, 1974.
- 25 Baker, I., Aschmann, S. M., Arey, J., and Atkinson, R.: Reactions of stabilized Criegee intermediates from the gas-phase reactions of O₃ with selected alkenes, *Int. J. Chem. Kinet.*, 34, 73–85, 2001.
- Barger, W. R. and Garrett, W. D.: Surface active organic material in the marine atmosphere, *J. Geophys. Res.*, 75, 4561–4566, 1970.
- 30 Bernatek, E., Hagen, H., and Ledaal, T.: Acidolysis of some stable ozonides, *Acta Chem. Scand.*, 21, 1555–1557, 1967.
- Bernatek, E. and Ledaal, T.: Solvolysis of ozonides, *Tetrahedron Lett.*, 1, 30–34, 1960.
- Bezdek, H. F. and Carlucci, A. F.: Concentration and removal of liquid microlayers from a

11152

- seawater surface by bursting bubbles, *Limnol. Oceanogr.*, 19, 126–132, 1974.
- Blanchard, D. C.: Sea-to-air transport of surface active material, *Science*, 146, 396–397, 1964.
- Broekhuizen, K. E., Thornberry, T., Kumar, P. P., and Abbatt, J. P. D.: Formation of cloud condensation nuclei by oxidative processing: unsaturated fatty acids, *J. Geophys. Res.*, 109, D24206, doi:10.1029/2004JD005298, 2004.
- 5 Bunnelle, W. H.: Preparation, properties, and reactions of carbonyl oxides, *Chem. Rev.*, 91, 335–362, 1991.
- Cheng, Y., Li, S.-M., Leithead, A., Brickell, P. C., and Leaitch, W. R.: Characterizations of *cis*-pinonic acid and *n*-fatty acids on fine aerosols in the Lower Fraser Valley during Pacific 2001
- 10 Air Quality Study, *Atmos. Environ.*, 38, 5789–5800, 2004.
- Chou, C.-M. and Hong, P.-D.: Nucleation, growth, fractal aggregation, and late-stage coarsening on structural development of polymer physical gels, *Macromolecules*, 37, 5596–5606, 2004.
- Crank, J.: *The Mathematics of Diffusion*, Clarendon Press, Oxford, 1975.
- 15 Criegee, R.: Mechanism of ozonolysis, *Agnew. Chem. internat. Edit.*, 14, 745–752, 1975.
- Criegee, R. and Wenner, G.: Ozonization of 1,2,3,4,5,6,7,8-octahydronaphthalene, *Liebigs Ann. Chem.*, 564, 9–15, 1949.
- Cronin, T. J. and Zhu, L.: Dye laser photolysis of *n*-pentanal from 280 to 330 nm, *J. Phys. Chem. A*, 102, 10274–10279, 1998.
- 20 Cruz, C. N. and Pandis, S. N.: A study of the ability of pure secondary organic aerosol to act as cloud condensation nuclei, *Atmos. Environ.*, 31, 2205–2214, 1997.
- Danckwerts, P. V.: *Gas-Liquid Reactions*, McGraw-Hill, New York, USA, 1970.
- Davidovits, P., Jayne, J. T., Duan, S. X., Worsnop, D. R., Zahniser, M. S., and Kolb, C. E.: Uptake of gas molecules by liquids: A model, *J. Phys. Chem.*, 95, 6337–6340, 1991.
- 25 de Gouw, J. A. and Lovejoy, E. R.: Reactive uptake of ozone by liquid organic compounds, *Geophys. Res. Lett.*, 25, 931–934, 1998.
- Decesari, S., Fuzzi, S., Facchini, M. C., Mircea, M., Emblico, L., Cavalli, F., Maenhaut, W., Chi, X., Schkolnik, G., Falkovich, A., Rudich, Y., Claeys, M., Pashynska, V., Vas, G., Kourtchev, I., Vermeylen, R., Hoffer, A., Andreae, M.O., Tagliavini, E., Moretti, F., and Artaxo, P.: Characterization of the organic composition of aerosols from Rondônia, Brazil, during the LBA-SMOCC
- 30 2002 experiment and its representation through model compounds, *Atmos. Chem. Phys.*, 6, 375–402, 2006.
- Demou, E., Visram, H., Donaldson, D. J., and Makar, P. A.: Uptake of water by organic films:

11153

- the dependence on the film oxidation state, *Atmos. Environ.*, 37, 3529–3537, 2003.
- Donaldson, D. J., Ravishankara, A. R., and Hanson, D. R.: Detailed study of $\text{HOCl} + \text{HCl} \rightarrow \text{Cl}_2 + \text{H}_2\text{O}$ in sulfuric acid, *J. Phys. Chem. A*, 101, 4717–4725, 1997.
- Duce, R. A., Mohnen, V. A., Zimmerman, P. R., Grosjean, D., Cautreels, W., Chatfield, R.,
- 5 Jaenicke, R., Ogren, J. A., Pellizzari, E. D., and Wallace, G. T.: Organic material in the global troposphere, *Rev. Geophys. Space Phys.*, 21, 921–952, 1983.
- Evlath, E. M., Melius, C. F., Rayez, M. T., Rayez, J. C., and Forst, W.: Theoretical characterization of the reaction of HO_2 with formaldehyde, *J. Phys. Chem.*, 97, 5040–5045, 1993.
- Facchini, M. C.: Organic compounds in clouds: Present knowledge and future perspectives, Newsletter of the International Atmospheric Chemistry Project, 23, 10–13, 2001.
- 10 Facchini, M. C., Mircea, M., Fuzzi, S., and Charlson, R. J.: Cloud albedo enhancement by surface-active solutes in growing droplets, *Nature*, 401, 257–259, 1999.
- Fenger, J.: Urban air quality, *Atmos. Environ.*, 33, 4877–4900, 1999.
- Fenske, J. D., Hasson, A. S., Paulson, S. E., Kuwata, K. T., Ho, A., and Houk, K. N.: The
- 15 pressure dependence of the OH radical yield from ozone-alkene reactions, *J. Phys. Chem. A*, 104, 7821–7833, 2000.
- Finlayson-Pitts, B. J. and Pitts Jr., J. N.: *Chemistry of the Upper and Lower Atmosphere*, Academic Press, NYC, USA, 1999.
- Fliszár, S., Gravel, D., and Cavaliere, E.: Étude quantitative des réactions d'ozonolyse II. Ozonation du *trans*-stilbène, *Can. J. Chem.*, 44, 1013–1019, 1966.
- 20 Fuzzi, S., Andreae, M. O., Huebert, B. J., Kulmala, M., Bond, T. C., Boy, M., Doherty, S. J., Guenther, A., Kanakidou, M., Kawamura, K., Kerminen, V.-M., Lohmann, U., Russell, L. M., and Pöschl, U.: Critical assessment of the current state of scientific knowledge, terminology, and research needs concerning the role of organic aerosols in the atmosphere, climate, and
- 25 global change, *Atmos. Chem. Phys.*, 6, 2017–2038, 2006.
- Goddard III, W. A., Dunning, J. T. H., Hunt, W. J., and Hay, P. J.: Generalized valence bond description of bonding in low-lying states of molecules, *Acc. Chem. Res.*, 6, 368–378, 1973.
- Graedel, T. E., Farrow, L. A., and Weber, T. A.: Kinetic studies of the photochemistry of the urban troposphere, *Atmos. Environ.*, 10, 1095–1116, 1976.
- 30 Greenwood, F. L.: Studies in ozonolysis. I. Action of ozone on solvents used in ozonation, *J. Org. Chem.*, 10, 414–418, 1945.
- Grosjean, D.: Formaldehyde and other carbonyls in Los Angeles ambient air, *Environ. Sci. Technol.*, 16, 254–262, 1982.

11154

- Guo, Z. G., Sheng, L. F., Feng, J. L., and Fang, M.: Seasonal variation of solvent extractable organic compounds in the aerosols in Qingdao, China, *Atmos. Environ.*, 37, 1825–1834, 2003.
- 5 Gutbrod, R., Kraka, E., Schindler, R. N., and Cremer, D.: Kinetic and theoretical investigation of the gas-phase ozonolysis of isoprene: carbonyl oxides as an important source of OH radicals in the atmosphere, *J. Am. Chem. Soc.*, 119, 7330–7342, 1997.
- Hahn, J.: Organic constituents of natural aerosols, *Ann. NY Acad. Sci.*, 338, 359–376, 1980.
- Hanson, D. R.: Surface-specific reactions on liquids, *J. Phys. Chem. B*, 101, 4998–5001, 1997.
- Hanson, D. R.: Reaction of ClONO₂ with H₂O and HCl in sulfuric acid and HNO₃/H₂SO₄/H₂O mixtures, *J. Phys. Chem. A*, 102, 4794–4807, 1998.
- 10 Hanson, D. R. and Lovejoy, E. R.: The reaction of ClONO₂ with submicrometer sulfuric acid aerosol, *Science*, 267, 1326–1328, 1995.
- Hanson, D. R. and Ravishankara, A. R.: Uptake of HCl and HOCl onto sulfuric acid: solubilities, diffusivities, and reaction, *J. Phys. Chem.*, 97, 12309–12319, 1993.
- 15 Hanson, D. R., Ravishankara, A. R., and Lovejoy, E. R.: Reaction of BrONO₂ with H₂O on submicron sulfuric acid aerosol and the implications for the lower stratosphere, *J. Geophys. Res.*, 101, 9063–9069, 1996.
- Harding, L. B. and Goddard III, W. A.: Mechanisms of gas-phase and liquid-phase ozonolysis, *J. Am. Chem. Soc.*, 100, 7180–7188, 1978.
- 20 Haywood, J. and Boucher, O.: Estimates of the direct and indirect radiative forcing due to tropospheric aerosols: A review, *Rev. Geophys. Space Phys.*, 38, 513–543, 2000.
- He, L.-Y., Hu, M., Huang, X.-F., Yu, B.-D., Zhang, Y.-H., and Liu, D.-Q.: Measurement of emissions of fine particulate organic matter from Chinese cooking, *Atmos. Environ.*, 38, 6557–6564, 2004.
- 25 Hearn, J. D., Lovett, A. J., and Smith, G. D.: Ozonolysis of oleic acid particles: evidence for a surface reaction and secondary reactions involving Criegee intermediates, *Phys. Chem. Chem. Phys.*, 7, 501–511, 2005.
- Hearn, J. D. and Smith, G. D.: A chemical ionization mass spectrometry method for the online analysis of organic aerosols, *Anal. Chem.*, 76, 2820–2826, 2004a.
- 30 Hearn, J. D. and Smith, G. D.: Kinetics and product studies for the ozonolysis reactions of organic particles using aerosol CIMS, *J. Phys. Chem. A*, 108, 1019–1029, 2004b.
- Hearn, J. D. and Smith, G. D.: Measuring rates of reaction in supercooled organic particles with implications for atmospheric aerosol, *Phys. Chem. Chem. Phys.*, 7, 2549–2551, 2005.

11155

- Heintzenberg, J.: Fine particles in the global troposphere, *Tellus*, 41B, 149–160, 1989.
- Hellén, H., Hakola, H., Reissell, A., and Ruuskanen, T. M.: Carbonyl compounds in boreal coniferous forest air in Hyytiälä, Southern Finland, *Atmos. Chem. Phys.*, 4, 1771–1780, 2004.
- 5 Herrmann, H., Wolke, R., Müller, K., Brüggemann, E., Gnauk, T., Barzaghi, P., Mertes, S., Lehmann, K., Massling, A., Birmili, W., Wiedensohler, A., Wieprecht, W., Acker, K., Jaeschke, W., Kramberger, H., Svrčina, B., Bächmann, K., Collett Jr., J. L., Galgon, D., Schwirn, K., Nowak, A., van Pinxteren, D., Plewka, A., Chemnitzer, R., Rüd, C., Hofmann, D., Tilgner, A., Diehl, K., Heinold, B., Hinneburg, D., Knoth, O., Sehili, A. M., Simmel, M., Wurzler, S.,
- 10 Majdik, Z., Mauersberger, G., and Müller, F.: FEBUKO and MODMEP: Field measurements and modelling of aerosol and cloud multiphase processes, *Atmos. Environ.*, 39, 4169–4183, 2005.
- Hiberty, P. C.: Mechanism of ozonolysis. Ab initio study of the primary ozonide and its cleavage to the Criegee intermediate, *J. Am. Chem. Soc.*, 98, 6088–6092, 1976.
- 15 Hildemann, L. M., Klinedinst, D. B., Klouda, G. A., Currie, L. A., and Cass, G. R.: Sources of urban contemporary carbon aerosol, *Environ. Sci. Technol.*, 28, 1565–1576, 1994.
- Hoffer, A., Gelencsér, A., Blazsó, M., Guyon, P., Artaxo, P., and Andreae, M. O.: Chemical transformations in organic aerosol from biomass burning, *Atmos. Chem. Phys. Discuss.*, 5, 8027–8054, 2005.
- 20 Hoffman, E. J. and Duce, R. A.: Organic carbon in the marine atmospheric particulate matter: Concentration and particle size distribution, *Geophys. Res. Lett.*, 4, 449–452, 1977.
- Horie, O., Neeb, P., Limbach, S., and Moortgat, G. K.: Formation of formic acid and organic peroxides in the ozonolysis of ethene with added water vapour, *Geophys. Res. Lett.*, 21, 1523–1526, 1994.
- 25 Huang, X.-F., He, L.-Y., Hu, M., and Zhang, Y.-H.: Annual variation of particulate organic compounds in PM_{2.5} in the urban atmosphere of Beijing, *Atmos. Environ.*, 40, 2449–2458, 2005.
- Hung, H.-M., Katrib, Y., and Martin, S. T.: Products and mechanisms of the reaction of oleic acid with ozone and nitrate radical, *J. Phys. Chem. A*, 109, 4517–4530, 2005.
- Inoue, T., Hisatsugu, Y., Yamamoto, R., and Suzuki, M.: Solid-liquid behavior of binary fatty acid mixtures 1. Oleic acid/stearic acid and oleic acid/behenic acid mixtures, *Chem. Phys. Lipids*, 127, 143–152, 2004.
- 30 Iwahashi, M., Kasahara, Y., Matsuzawa, H., Yagi, K., Nomura, K., Terauchi, H., Ozaki, Y., and Suzuki, M.: Self-diffusion, dynamical molecular conformation, and liquid structures of

11156

- n*-saturated and unsaturated fatty acids, *J. Phys. Chem. B*, 104, 6186–6194, 2000.
- Iwahashi, M., Suzuki, M., Czarnecki, M. A., Liu, Y., and Ozaki, Y.: Near-IR molar absorption coefficient for the OH-stretching mode of *cis*-9-octadecenoic acid and dissociation of the acid dimers in the pure liquid state, *J. Chem. Soc. Faraday Trans.*, 91, 697–701, 1995.
- 5 Iwahashi, M., Yamaguchi, Y., Kato, T., Horiuchi, T., Sakurai, I., and Suzuki, M.: Temperature dependence of molecular conformation and liquid structure of *cis*-9-octadecenoic acid, *J. Phys. Chem.*, 95, 445–451, 1991.
- Johnson, B. T., Shine, K. P., and Forster, P. M.: The semi-direct aerosol effect: Impact of absorbing aerosols on marine stratocumulus, *Q. J. R. Meteorol. Soc.*, 130, 1407–1422, 2004.
- 10 Kanakidou, M., Seinfeld, J. H., Pandis, S. N., Barnes, I., Dentener, F. J., Facchini, M. C., Van Dingenen, R., Ervens, B., Nenes, A., Nielson, C. J., Swietlicki, E., Putaud, J. P., Balkanski, Y., Fuzzi, S., Horth, J., Moortgat, G. K., Winterhalter, R., Myhre, C. E. L., Tsigaridis, K., Vignati, E., Stephanou, E. G., and Wilson, J.: Organic aerosol and global climate modelling: a review, *Atmos. Chem. Phys.*, 5, 1053–1123, 2005.
- 15 Kärcher, B. and Koop, T.: The role of organic aerosols in homogeneous ice formation, *Atmos. Chem. Phys.*, 5, 703–714, 2005.
- Katrib, Y., Biskos, G., Buseck, P. R., Davidovits, P., Jayne, J. T., Mochida, M., Wise, M. E., Worsnop, D. R., and Martin, S. T.: Ozonolysis of mixed oleic-acid/stearic-acid particles: Reaction kinetics and chemical morphology, *J. Phys. Chem. A*, 109, 10910–10919, 2005a.
- 20 Katrib, Y., Martin, S. T., Hung, H.-M., Rudich, Y., Zhang, H., Slowik, J. G., Davidovits, P., Jayne, J. T., and Worsnop, D. R.: Products and mechanisms of ozone reactions with oleic acid for aerosol particles having core-shell morphologies, *J. Phys. Chem. A*, 108, 6686–6695, 2004.
- Katrib, Y., Martin, S. T., Rudich, Y., Davidovits, P., Jayne, J. T., and Worsnop, D. R.: Density changes of aerosol particles as a result of chemical reaction, *Atmos. Chem. Phys.*, 5, 275–291, 2005b.
- 25 Ketsseridis, G. and Eichmann, R.: Organic compounds in aerosol samples, *Pure Appl. Geophys.*, 116, 274–282, 1978.
- Knopf, D. A., Anthony, L. M., and Bertram, A. K.: Reactive uptake of O₃ by multicomponent and multiphase mixtures containing oleic acid, *J. Phys. Chem. A*, 109, 5579–5589, 2005.
- 30 Köhler, H.: The nucleus in and the growth of hygroscopic particles, *Trans. Faraday Soc.*, 32, 1152–1161, 1936.
- Kolb, C. E., Davidovits, P., Jayne, J. T., Shi, Q., and Worsnop, D. R.: Kinetics of trace gas uptake by liquid surfaces, *Prog. React. Kinet. Mec.*, 27, 1–46, 2002.

11157

- Kumar, P. P., Broekhuizen, K., and Abbatt, J. P. D.: Organic acids as cloud condensation nuclei: Laboratory studies of highly soluble and insoluble species, *Atmos. Chem. Phys.*, 3, 509–520, 2003.
- 5 LaFranchi, B. W. and Petrucci, G. A.: Photoelectron resonance capture ionization (PERCI): A novel technique for the soft-ionization of organic compounds, *J. Am. Soc. Mass Spectrom.*, 15, 424–430, 2004.
- LaFranchi, B. W., Zahardis, J., and Petrucci, G. A.: Photoelectron resonance capture ionization mass spectrometry: a soft ionization source for mass spectrometry of particle-phase organic compounds, *Rapid Commun. Mass Spectrom.*, 18, 2517–2521, 2004.
- 10 Ledea, O., Díaz, M., Molerio, J., Jardines, D., Rosado, A., and Correa, T.: ¹H-NMR spectroscopy study of oleic acid and methyl oleate ozonation in different reaction conditions, *Revista CENIC Ciencias Químicas*, 34, 3–8, 2003.
- Limbeck, A. and Puxbaum, H.: Organic acids in continental background aerosols, *Atmos. Environ.*, 33, 1847–1852, 1999.
- 15 Lohmann, U. and Feichter, J.: Global indirect aerosol effects: a review, *Atmos. Chem. Phys.*, 5, 715–737, 2005.
- Lovejoy, E. R., Huey, L. G., and Hanson, D. R.: Atmospheric fate of CF₃OH 2: Heterogeneous reaction, *J. Geophys. Res.*, 100, 18775–18780, 1995.
- Mag, T.: Canola and Rapeseed. Production, Chemistry, Nutrition, and Processing Technology, Avi Book, Van Nostrand Reinhold, NY, USA, 1990.
- 20 Marty, J. C., Saliot, A., Buat-Ménard, P., Chesselet, R., and Hunter, K. A.: Relationship between the lipid compositions of marine aerosols, the sea surface microlayer, and subsurface water, *J. Geophys. Res.*, 84, 5707–5716, 1979.
- Mayol-Bracero, O. L., Guyon, P., Graham, B., Roberts, G., Andreae, M. O., Decesari, S., Facchini, M. C., Fuzzi, S., and Artaxo, P.: Water-soluble organic compounds in biomass burning over Amazonia 2. Apportionment of the chemical composition and importance of the polyacidic fraction, *J. Geophys. Res.*, 107(D20), 8091, doi:10.1029/2001JD000522, 2002.
- Mayol-Bracero, O. L., Rosario, O., Corrigan, C. E., Morales, R., Torres, I., and Pérez, V.: Chemical characterization of submicron organic aerosols in the tropical trade winds of the Caribbean using gas chromatography/mass spectrometry, *Atmos. Environ.*, 35, 1735–1745, 2001.
- 30 McFiggans, G., Artaxo, P., Baltensperger, U., Coe, H., Facchini, M. C., Feingold, G., Fuzzi, S., Gysel, M., Laaksonen, A., Lohmann, U., Mentel, T. F., Murphy, D. M., O'Dowd, C. D., Snider, J. R., and Weingartner, E.: The effect of physical and chemical aerosol properties on warm

11158

- cloud droplet activation, *Atmos. Chem. Phys.*, 6, 2593–2649, 2006.
- Moise, T. and Rudich, Y.: Reactive uptake of ozone by proxies for organic aerosols: Surface versus bulk processes, *J. Geophys. Res.*, 105, 14 667–14 676, 2000.
- Moise, T. and Rudich, Y.: Uptake of Cl and Br by organic surfaces – a perspective on organic aerosols processing by tropospheric oxidants, *Geophys. Res. Lett.*, 28, 4083–4086, 2001.
- Moise, T. and Rudich, Y.: Reactive uptake of ozone by aerosol-associated fatty acids: kinetics, mechanism, and products, *J. Phys. Chem. A*, 106, 6469–6476, 2002.
- Moise, T., Talukdar, R. K., Frost, G. J., Fox, R. W., and Rudich, Y.: Reactive uptake of NO₃ by liquid and frozen organics, *J. Geophys. Res.*, 107(D2), AAC6/1–AAC6/9, doi:10.1029/2001JD000334, 2002.
- Morris, J. W., Davidovits, P., Jayne, J. T., Jimenez, J. L., Shi, Q., Kolb, C. E., Worsnop, D. R., Barney, W. S., and Cass, G.: Kinetics of submicron oleic acid aerosols with ozone: a novel mass spectrometric technique, *Geophys. Res. Lett.*, 29, 71/71–71/74, 2002.
- Moussa, S. G., El-Fadel, M., and Saliba, N. A.: Seasonal, diurnal and nocturnal behaviors of lower carbonyl compounds in the urban environment of Beirut, Lebanon, *Atmos. Environ.*, 40, 2459–2468, 2006.
- Murray, R. W.: The mechanism of ozonolysis, *Acc. Chem. Res.*, 1, 313–320, 1968.
- Murray, R. W. and Williams, G. J.: Ozonolysis. Steric effects in the aldehyde, *J. Org. Chem.*, 34, 1891–1895, 1969.
- Mysak, E. R., Wilson, K. R., Jimenez-Cruz, M., Ahmed, M., and Baer, T.: Synchrotron radiation based aerosol time-of-flight mass spectrometry for organic constituents, *Anal. Chem.*, 77, 5953–5960, 2005.
- Neeb, P., Horie, O., and Moortgat, G. K.: The nature of the transitory product in the gas-phase ozonolysis of ethene, *Chem. Phys. Lett.*, 246, 150–156, 1995.
- Neeb, P., Horie, O., and Moortgat, G. K.: Gas-phase ozonolysis of ethene in the presence of hydroxylic compounds, *Int. J. Chem. Kinet.*, 28, 721–730, 1996.
- Neeb, P., Horie, O., and Moortgat, G. K.: The ethene – ozone reaction in the gas phase, *J. Phys. Chem. A*, 102, 6778–6785, 1998.
- Nishikawa, A., Yamada, K., Matsutani, S., Higo, M., Kigawa, H., and Inagaki, T.: Structure of ozonolysis products of methyl oleate obtained in a carboxylic acid medium, *J. Am. Oil Chem. Soc.*, 72, 735–740, 1995.
- Novakov, T. and Corrigan, C. E.: Cloud condensation nucleus activity of the organic component of biomass smoke particles, *Geophys. Res. Lett.*, 23, 2141–2144, 1996.

11159

- O'Dowd, C. D., Facchini, M. C., Cavalli, F., Ceburnis, D., Mircea, M., Decesari, S., Fuzzi, S., Yoon, Y. J., and Putaud, J.-P.: Biogenically driven organic contribution to marine aerosol, *Nature*, 431, 676–680, 2004.
- Parrondo, R. M., Karafiloglou, P., Pappalardo, R. R., and Marcos, E. S.: Calculation of the weights of resonance structures of molecules in solution, *J. Phys. Chem.*, 99, 6461–6467, 1995.
- Pio, C., Alves, C., and Duarte, A.: Organic components of aerosols in a forested area of central Greece, *Atmos. Environ.*, 35, 389–401, 2001.
- Pryde, E. H., Moore, D. J., and Cowan, J. C.: Hydrolytic, reductive and pyrolytic decomposition of selected ozonolysis products. Water as an ozonization medium, *J. Am. Oil Chem. Soc.*, 45, 888–894, 1968.
- Raymond, T. M. and Pandis, S. N.: Cloud activation of single-component organic aerosol particles, *J. Geophys. Res.*, 107(D24), 4787, doi:10.1029/2002JD002159, 2002.
- Rebrovic, L.: The peroxidic species generated by ozonolysis of oleic acid or methyl oleate in a carboxylic acid medium, *J. Am. Oil Chem. Soc.*, 69, 159–165, 1992.
- Reid, J. S., Koppmann, R., and Eleuterio, D. P.: A review of biomass burning emissions, part II: Intensive physical properties of biomass burning particles, *Atmos. Chem. Phys.*, 5, 799–825, 2005.
- Rogge, W. F., Hildemann, L. M., Mazurek, M. A., and Cass, G. R.: Sources of fine organic aerosol. 1. Charbroilers and meat cooking operations, *Environ. Sci. Technol.*, 25, 1112–1125, 1991.
- Rogge, W. F., Hildemann, L. M., Mazurek, M. A., Cass, G. R., and Simoneit, B. R. T.: Sources of fine organic aerosol. 4. Particulate abrasion products from leaf surfaces of urban plants, *Environ. Sci. Technol.*, 27, 2700–2711, 1993.
- Rogge, W. F., Medeiros, P. M., and Simoneit, B. R. T.: Organic marker compounds for surface soil and fugitive dust from open lot dairies and cattle feedlots, *Atmos. Environ.*, 40, 27–49, 2006.
- Rudich, Y.: Laboratory perspectives on the chemical transformations of organic matter in atmospheric particles, *Chem. Rev.*, 103, 5097–5124, 2003.
- Schauer, J. J., Kleeman, M. J., Cass, G. R., and Simoneit, B. R. T.: Measurement of emissions from air pollution sources. 1. C₁ through C₂₉ organic compounds from meat charbroiling, *Environ. Sci. Technol.*, 33, 1566–1577, 1999.
- Seidl, W.: Model for a surface film of fatty acids on rain water and aerosol particles, *Atmos.*

11160

- Environ., 34, 4917–4932, 2000.
- Selçuki, C. and Aviyente, V.: A DFT study of carbonyl oxide and its methyl-substituted analogues in solution, *Chem. Phys. Lett.*, 288, 669–676, 1998.
- Shi, Q., Davidovits, P., Jayne, J. T., Worsnop, D. R., and Kolb, C. E.: Uptake of gas-phase ammonia. 1. Uptake by aqueous surfaces as a function of pH, *J. Phys. Chem. A*, 103, 8812–8823, 1999.
- Simoneit, B. R. T.: Application of molecular marker analysis to vehicular exhaust for source reconciliations, *Intern. J. Environ. Anal. Chem.*, 22, 203–233, 1985.
- Simoneit, B. R. T.: Characterization of organic constituents in aerosols in relation to their origin and transportation: A review, *Intern. J. Environ. Anal. Chem.*, 23, 207–237, 1986.
- Simoneit, B. R. T., Cox, R. E., and Standley, L. J.: Organic matter of the troposphere – IV. Lipids in Harmattan aerosols of Nigeria, *Atmos. Environ.*, 22, 983–1004, 1988.
- Simoneit, B. R. T., Crisp, P. T., Mazurek, M. A., and Standley, L. J.: Composition of extractable organic matter of aerosols from the Blue Mountains and southeast coast of Australia, *Environ. Int.*, 17, 405–419, 1991.
- Simoneit, B. R. T. and Mazurek, M. A.: Organic matter of the troposphere – II. Natural background of biogenic lipid matter in aerosols over the rural western United States, *Atmos. Environ.*, 16, 2139–2159, 1982.
- Smith, G. D., Woods III, E., DeForest, C. L., Baer, T., and Miller, R. E.: Reactive uptake of ozone by oleic acid aerosol particles: Application of single-particle mass spectrometry to heterogeneous reaction kinetics, *J. Phys. Chem. A*, 106, 8085–8095, 2002.
- Sturrock, M. G., Cline, E. L., and Robinson, K. R.: The ozonation of phenanthrene with water as participating solvent, *J. Org. Chem.*, 28, 2340–2343, 1963.
- Sun, J. and Ariya, P. A.: Atmospheric organic and bio-aerosol as cloud condensation nuclei (CCN): A review, *Atmos. Environ.*, 40, 795–820, 2006.
- Sykes, D. C., Woods III, E., Smith, G. D., Baer, T., and Miller, R. E.: Thermal vaporization-vacuum ultraviolet laser ionization time-of-flight mass spectrometry of single aerosol particles, *Anal. Chem.*, 74, 2048–2052, 2002.
- Thornberry, T. and Abbatt, J. P. D.: Heterogeneous reaction of ozone with liquid unsaturated fatty acids: detailed kinetics and gas-phase product studies, *Phys. Chem. Chem. Phys.*, 6, 84–93, 2004.
- Tobias, H. J., Docherty, K. S., Beving, D. E., and Ziemann, P. J.: Effect of relative humidity on the chemical composition of secondary organic aerosol formed from the reactions of 1-

11161

- tetradecene and O₃, *Environ. Sci. Technol.*, 34, 2116–2125, 2000.
- Tobias, H. J. and Ziemann, P. J.: Compound identification in organic aerosols using temperature-programmed thermal desorption particle beam mass spectrometry, *Anal. Chem.*, 71, 3428–3435, 1999.
- Tobias, H. J. and Ziemann, P. J.: Thermal desorption mass spectrometric analysis of organic aerosol formed from reactions of 1-tetradecene and O₃ in the presence of alcohols and carboxylic acids, *Environ. Sci. Technol.*, 34, 2105–2115, 2000.
- Tobias, H. J. and Ziemann, P. J.: Kinetics of the gas-phase reactions of alcohols, aldehydes, carboxylic acids, and water with the C13 stabilized Criegee intermediate from the ozonolysis of 1-tetradecene, *J. Phys. Chem. A*, 105, 6129–6135, 2001.
- Toyota, K., Kanaya, Y., Takahashi, M., and Akimoto, H.: A box model study on photochemical interactions between VOCs and reactive halogen species in the marine boundary layer, *Atmos. Chem. Phys.*, 4, 1961–1987, 2004.
- Twomey, S.: The nuclei of natural cloud formation, part II: The supersaturation in natural clouds and the variation of cloud droplet concentration, *Geofis. Pure Appl.*, 43, 243–248, 1959.
- Utter, R. G., Burkholder, J. B., Howard, C. J., and Ravishankara, A. R.: Measurement of the mass accommodation coefficient of ozone on aqueous surfaces, *J. Phys. Chem.*, 96, 4973–4979, 1992.
- Wadia, Y., Tobias, D. J., Stafford, R., and Finlayson-Pitts, B. J.: Real-time monitoring of the kinetics and gas-phase products of the reaction of ozone with an unsaturated phospholipid at the air-water interface, *Langmuir*, 16, 9321–9330, 2000.
- Wadt, W. R. and Goddard III, W. A.: The electronic structure of the Criegee intermediate. Ramifications for the mechanism of ozonolysis, *J. Am. Chem. Soc.*, 97, 3004–3021, 1975.
- Wolff, S., Boddenberg, A., Thamm, J., Turner, W. V., and Gäb, S.: Gas-phase ozonolysis of ethene in the presence of carbonyl-oxide scavengers, *Atmos. Environ.*, 31, 2965–2969, 1997.
- Woods III, E., Smith, G. D., Dessiaterik, Y., Baer, T., and Miller, R. E.: Quantitative detection of aromatic compounds in single aerosol particle mass spectrometry, *Anal. Chem.*, 73, 2317–2322, 2001.
- Woods III, E., Smith, G. D., Miller, R. E., and Baer, T.: Depth profiling of heterogeneously mixed aerosol particles using single-particle mass spectrometry, *Anal. Chem.*, 74, 1642–1649, 2002.
- Worsnop, D. R., Morris, J. W., Shi, Q., Davidovits, P., and Kolb, C. E.: A chemical kinetic

11162

model for reactive transformations of aerosol particles, *Geophys. Res. Lett.*, 29, 57/51–57/53, doi:10.1029/2002GL015542, 2002.

- Yu, S.: Role of organic acids (formic, acetic, pyruvic and oxalic) in the formation of cloud condensation nuclei (CCN): a review *Atmos. Res.*, 53, 185–217, 2000.
- 5 Zahardis, J., LaFranchi, B. W., and Petrucci, G. A.: Photoelectron resonance capture ionization-aerosol mass spectrometry of the ozonolysis products of oleic acid particles: Direct measure of higher molecular weight oxygenates, *J. Geophys. Res.*, 110, D08307, doi:10.1029/2004JD005336, 2005.
- 10 Zahardis, J., LaFranchi, B. W., and Petrucci, G. A.: Direct observation of polymerization in the oleic acid-ozone heterogeneous reaction system by photoelectron resonance capture ionization aerosol mass spectrometry, *Atmos. Environ.*, 40, 1661–1670, 2006a.
- Zahardis, J., LaFranchi, B. W., and Petrucci, G. A.: The heterogeneous reaction of particle-phase methyl esters and ozone elucidation by photoelectron resonance capture ionization: Direct products of ozonolysis and secondary reactions leading to the formation of ketones, *Int. J. Mass Spectrom.*, 253, 38–47, 2006b.
- 15 Zelikman, E. S., Yur'ev, Y. N., Berezova, L. V., and Tsyksovskii, V. K.: Ozonolysis of olefins in the presence of aliphatic alcohols and acids, *Zh. Organ. Khim.*, 7, 633–636, 1971.
- Ziemann, P. J.: Formation of alkoxyhydroperoxy aldehydes and cyclic peroxyhemiacetals from reactions of cyclic alkenes with O₃ in the presence of alcohols, *J. Phys. Chem. A*, 107, 2048–2060, 2003.
- 20 Ziemann, P. J.: Aerosol products, mechanisms, and kinetics of heterogeneous reactions with oleic acid in pure and mixed particles, *Faraday Discuss.*, 130, 469–490, 2005.

11163

Table 1. Products observed in the ozonolysis of OL particles and coatings.

OL dimension (diameter or thickness)	O ₃ conc (molecules cm ⁻³)	reacn time (s)	Aerosol Experiments		Coated wall experiments				Carbon-based yield of products (%)					Ref.	
			OL conc (molecules cm ⁻³)	OL conc (molecules particle ⁻¹)	flow (cm ³ s ⁻¹)	no. of molec of OL	no. of molecules of O ₃ (mg/d quantity)	molar ratio of O ₃ to OL	O ₃ expos. (atm s)	NN	OX	AA	NA		other
200–600 nm	2.5×10 ¹⁴	7	<2×10 ^{12b}	(8–200)×10 ⁶				>10 ²	7×10 ⁻⁵	n/a	n/a	n/a	n/a		Morris et al. (2002)
10 ³ μm	1.0×10 ¹⁴	0.1			50–200	1.9×10 ²¹	1.0×10 ¹⁵	10 ⁻⁶	4×10 ⁻⁷	25 ^c	n/a	P	P		Moise and Rudich (2000, 2002)
1.4–4.9 μm	3.4×10 ¹⁵	8	<1×10 ^{14d}	(3–100)×10 ⁹				>30	1×10 ⁻³	n/a	P	n/a	n/a		Smith et al. (2002)
ca. 50 μm	10 ^{11–10¹²}	>0.1			1.8	2×10 ²¹	>2×10 ¹⁰	>10 ⁻¹¹	>10 ⁻⁹	25 ^c	n/a	n/a	n/a		Thornberry and Abbott (2004)
2–30 nm	2.5×10 ¹⁴	3	3×10 ^{18e}	3×10 ^{6e}				10 ⁶	1×10 ⁻⁵	0 ^f	35 ^g	2 ^g	2 ^g	35% yield of C ₄ H ₈ O ₂ products; 25% increase in particle density	Kaltrib et al. (2004, 2005b)
ca. 100 μm	10 ^{14–10¹⁶}	300			17	2.1×10 ¹⁷	3×10 ^{19g}	140 ^g	8×10 ^{-2g}	n/a	n/a	n/a	n/a	increase in water uptake at 95% relative humidity	Asad et al. (2004)
0.6–1.0 μm	2.5×10 ¹⁵	4	<5×10 ^{13h}	5×10 ⁸				>50	4×10 ⁻⁴	42 ⁱ	42 ⁱ	6	9 ⁱ	1% yield of OOA	Hearn and Smith (2004b)
161 nm	1.0×10 ¹⁶	300	<4×10 ^{15b}	4×10 ⁶				>2×10 ⁶	4×10 ⁻¹	n/a	n/a	n/a	n/a	increase in CCN activity but only for high ozone exposure	Brosthusen et al. (2004)
155 nm	4.5×10 ¹⁵	10	4×10 ¹¹	4×10 ⁶				1×10 ⁴	2×10 ⁻³	P	P	P	P	cyclic oxygenates having oxygen moieties, including SO and cyclic geminal diperoxides	Zahardis et al. (2005)
0.6–1.2 μm	2.5×10 ¹⁴ to 2.5×10 ¹⁵	4	<5×10 ^{13h,k}	5×10 ⁸				>50 ^h	4×10 ^{-4j}	n/a	n/a	n/a	n/a	uptake results suggest 36% OL loss because of reactions with Cl	Hearn et al. (2005)
polydisperse, submicron	7.0×10 ¹³	300	4×10 ¹²	n/a				18	8×10 ⁻⁴	0 ^f	P	P	0	major products include ACOAH, SO, ALDAH, and monocarboxylic acids	Ziemann (2005)
0.5–3 nm	7.5×10 ¹⁵	2000			1.7	1.9×10 ¹⁸	3×10 ¹⁹	16	1	30 ^f	14	6	7	major yield of ester polymerization products of high molecular weight (specifically, ACOAH); 1% yield of octanoic acid	Hung et al. (2005)

Key. ^a The designation "n/a" indicates that the analysis was not performed for these chemical species. "P" indicates the chemical species was present but its yield not quantified. Key: NN, nonanal; OX, 9-oxononanoic acid; AA, azelaic acid; NA, nonanoic acid. All other abbreviations correspond to the text and are compiled in the Appendix. ^b Assumption is made of an upper limit of 10⁴ particles cm⁻³ based on use of electrostatic classification of a polydisperse source. ^c Gas-phase NN. ^d Assumption is made of an upper limit of 10³ particles cm⁻³ based upon use of vibrating orifice generator. ^e Results shown are for a 30 nm coating. ^f Condensed-phase NN. ^g A range of ozone concentrations was used. Results are summarized for 6.5×10¹⁴ molecules of O₃ cm⁻³. ^h Assumption is made of an upper limit of 10⁵ particles cm⁻³ based upon use of a Meinhard TR-30-A1 polydisperse source. ⁱ These yields are tentative because relative detection sensitivities are assumed. See original publication. ^j Combined condensed-phase and gas-phase NN. ^k 800 nm particles and 2.5×10¹⁵ molecules of O₃ cm⁻³ are employed for these calculations. (Table adapted from Hung et al., 2005)

11164

Table 2. Reactive uptake of ozone by OL, other FA and related compounds, and select mixed particles and coatings.

	Hearn and Smith (2004b)	Morris et al. (2002)	Smith et al. (2002)	Hearn et al. (2005)	Ziemann (2005)	Katrib et al. (2005a)	Knopf et al. (2005)	Moise and Rudich (2002)	Thornberry and Abbatt (2004)
Method	AFT CIMS	AFT AMS	AFT Single particle MS	AFT CIMS	Env. Chamber TDPBMS	AFT AMS	CFT CIMS (O ₃)	CFT CIMS (O ₃)	CFT CIMS (O ₃)
OL	(7.5±1.2)×10 ⁻⁴	(1.6±0.2)×10 ⁻³	(0.99±0.09)– (7.3±1.5)×10 ^{-3c} (5.8–8.8)×10 ^{-3d}	(1.38±0.06)×10 ⁻³ (8.8±0.5)×10 ^{-4e}	(1.3±0.2)×10 ⁻³	(1.25±0.2)×10 ⁻³	(0.64±0.05)×10 ⁻⁴ s (7.9±0.3)×10 ⁻⁴ l	(8.3±0.02)×10 ⁻⁴ s (5.2±0.1)×10 ⁻⁵ s	(8.0±1.0)×10 ⁻⁴
LA	(1.1±0.2)×10 ⁻³							(1.2±0.2)×10 ⁻³ l (1.4±0.1)×10 ⁻³ s	(1.3±0.1)×10 ⁻³
LN									
MOL				(1.23±0.10)×10 ⁻³					(1.8±0.2)×10 ⁻³
OL/SA						(1.25±0.2)– (0.6±0.15)×10 ^{-3f} (0.15±0.1)×10 ^{-3g}			
OL/C12							(4–7.2)×10 ⁻⁴ l (0.2– 1.7)×10 ⁻⁴ s – l		
OL/C14							(4–7.2)×10 ⁻⁴ l (0.2– 1.7)×10 ⁻⁴ s – l		
OL/C16					(0.13±0.1)×10 ⁻³ (0.25±0.2)×10 ⁻³ (1.1±0.4)×10 ⁻³				
Oleic/C17									
Oleic/DOS								(1.6–6.9)×10 ⁻⁵	
meat-cooking acids ^h									
d _p (µm)	0.8–1.5 ^b	0.2–0.6	0.680–2.45	0.6–1.2 (OL) 0.6–1.110 (MOL)	0.02–0.5	0.300 (mobility)			0.6 mm film (ave.)
max O ₃ exp. (atm s) ⁱ	5×10 ⁻⁴	~1×10 ⁻⁴	1×10 ⁻³	~5×10 ⁻⁴	~1.4×10 ⁻³	3.00×10 ⁻⁴	~1.5×10 ⁻⁸	~2.4×10 ⁻⁹	~2.1×10 ⁻⁸ (OL)

Key ^a Polydisperse aerosols with a mean diameter of 800 nm. ^b The symbol (–) indicates we estimated the maximum exposure of ozone from data presented in the original work. ^c This corresponds with a range of monodisperse particles, respectively, from 2.45 µm to 680 nm with other values of γ for different diameter particles given in the original work. ^d These are the corrected values of γ accounting for the diffusion of OL; see original work and Sect. 4.4.2.2 in this work for more details. ^e This is a corrected value accounting for OL loss via secondary chemistry; see the original work and Sect. 4.4.3.1 in this work for more details. ^f These values correspond to OL/SA from 100/0 to 60/40, by weight. ^g These values correspond to OL/SA from 50/50 to 0/100 by weight. ^h See original work and Sect. 4.4.3.4 in this work for details on the multicomponent coatings.

11165

Table 3. The limiting cases of O₃ uptake by particulate OL. Derivation of γ for Cases 1–3 is given in the original works Worsnop et al., 2002; Smith et al., 2002; Hearn et al., 2005) and details on Case 4 are given by Worsnop et al. (2002). An outline of the resistor model is given in Sect. 4.2 of this report; a summary of the approximations of these Cases is given in Sect. 4.3.

Limiting cases	$[OL]/[OL]_{t=0}$	γ
Case 1: Rapid diffusion of ozone throughout the particle	$\exp(-H k_2 P_{O_3} t)$	$\frac{4 H R T r k_2 [OL]}{3 \bar{c}}$
Case 2: Reaction limited by ozone diffusion. (A near surface reaction.)	$\left(1 - \frac{3 H (D k_2)^{1/2} P_{O_3} t}{2 r ([OL])^{1/2}}\right)^2$	$\frac{4 H R T (D k_2 [OL])^{1/2}}{\bar{c}}$
Case 3: Reaction at the surface	$\exp\left(\frac{-3 \delta^2 H k_2^{surf} P_{O_3} t}{r}\right)$	$\frac{4 H R T \delta^2 k_2^{surf} [OL]}{\bar{c}}$
Case 4: Uptake limited by OL diffusion	$\exp\left(\frac{-12 D_{OL} t}{r^2}\right)$	$\frac{16 D [OL]}{P_{O_3} \bar{c} r}$

11166

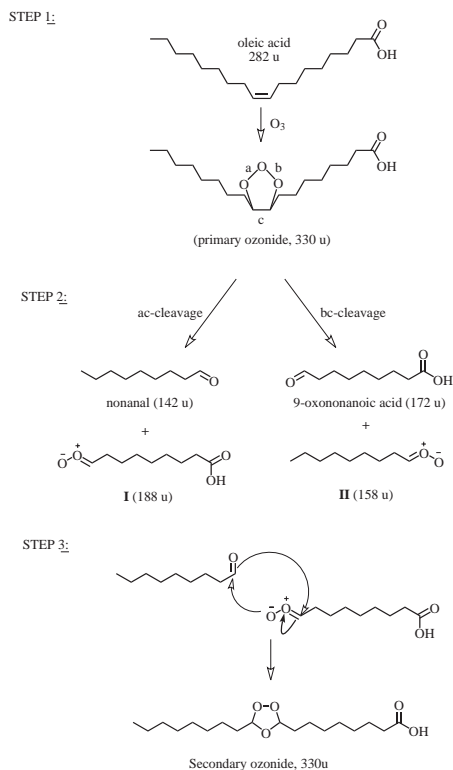


Fig. 1. Three-step reaction sequence of ozonolysis adapted to OL. Step 1: The formation of the PO; Step 2: Decomposition of the PO; Step 3: An example of dipolar cycloaddition (for ac-cleavage route products) of CI (I) with nonanal.

11167

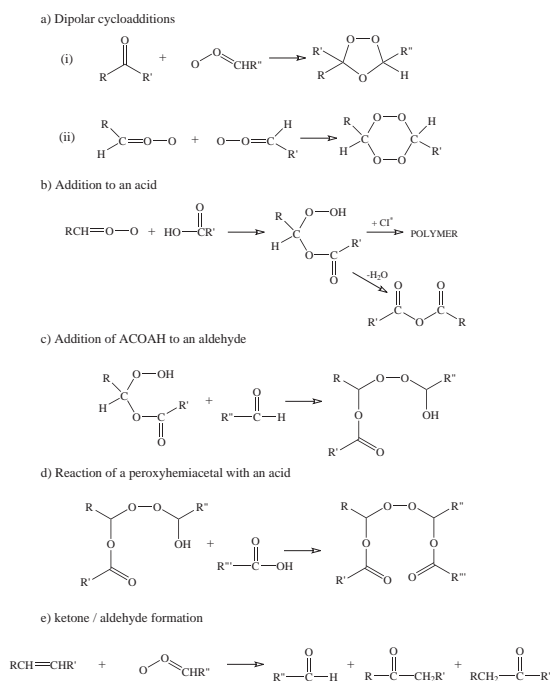


Fig. 2. Secondary chemistry arising from CI: **(a)** (i) Dipolar cycloaddition of CI with a carbonyl containing species forming a SO and (ii) Dipolar addition of two CI forming a cyclic geminal diperoxide (1, 2, 4-trioxolane); **(b)** Addition of CI to an organic acid leading to ACOAH (* when R or R' contains a carbonyl group polymer propagation can occur); **(c)** Reaction of ACOAH with an aldehyde forming a peroxyhemiacetal; **(d)** Further reaction of a peroxyhemiacetal with an organic acid forming a bis(α -acyloxy- α -alkyl) peroxide; **(e)** CI reaction with an unsaturated compound forming a ketone.

11168

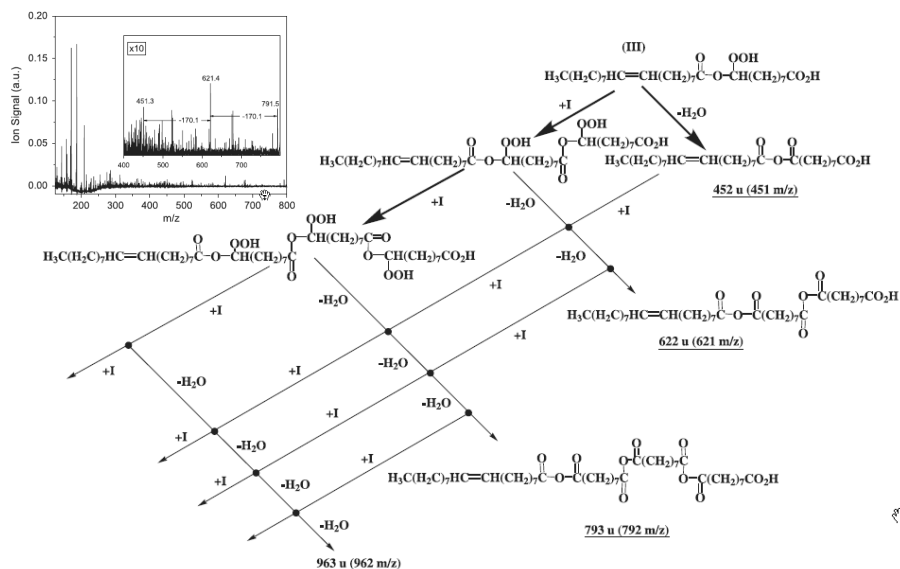


Fig. 3. The formation of peroxidic polymers (ACOAH and corresponding polyanhydrides). Depicted are products arising from the addition of Cl (I) (see Fig. 1) with OL. Underlined are the products directly observed in the PERCI mass spectrum shown in the inset (adapted from Zahardis et al., 2006a).

11169

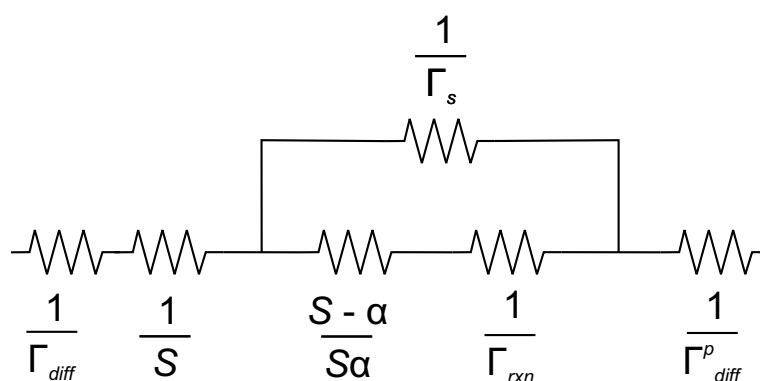


Fig. 4. The resistor model, an electric circuit analogue applied to reactive uptake microphysics of organic aerosols. In this model microphysical processes are represented as resistances, with gas-phase diffusion (Γ_{diff}), surface reaction (Γ_s), mass accommodation (α), chemical reaction within the particle (Γ_{rxn}), diffusion-limited mixing within particle (Γ_{diff}^p), and the adsorption coefficient (S) depicted.

11170

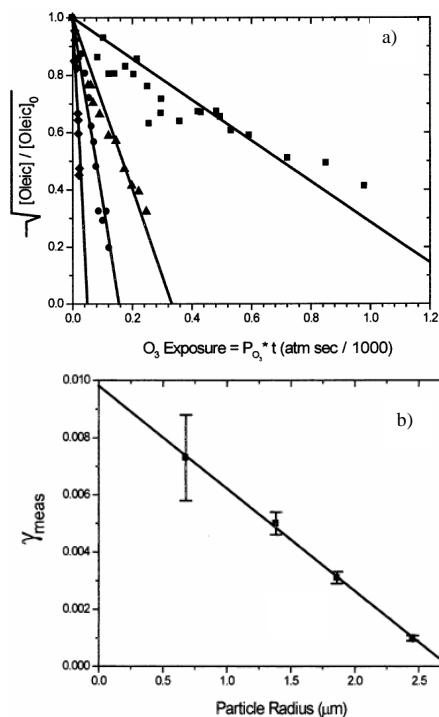


Fig. 5. OL decay profiles as measured by single-particle MS. **(a)** Decay profiles of four particle sizes: (◆) 680 nm, (●) 1.38 μm, (▲) 1.86 μm, (■) 2.45 μm. **(b)** Radial dependence evidenced in reactive uptake coefficients, although no radial dependency is predicted by Case 2 as discussed in Sect. 4.4.2.2 (from Smith et al., 2002).

11171

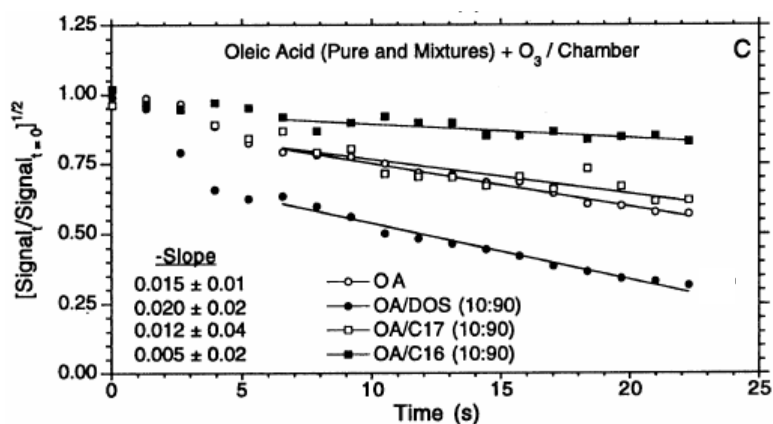


Fig. 6. Real-time TDPBMS signal of oleic acid (oleic acid is denoted OA in figure, while DOS, C17 and C16 correspond to our notation) decay for pure and mixed particles undergoing ozonolysis as discussed, respectively, in Sects. 4.4.2.4 and 4.4.3.3. Longer times of reaction are shown in Fig. 10 of the original work (adapted from Ziemann, 2005).

11172

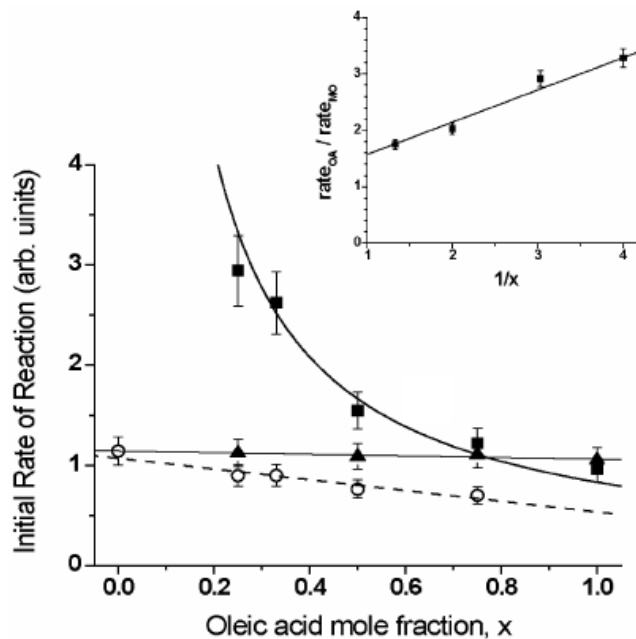


Fig. 7. Initial rates of reaction for internally mixed particles of OL (■) and MOL (○). These initial rates are normalized to the rate of pure OL particles. Rates of internally mixed OL/*n*-hexadecane (▲) are shown for comparison. The increase in the OL decay rate at lower mole fractions of OL results from greater contributions to OL loss from reactions with Cl. The inset shows the ratio of the rates (with OA denoting oleic acid and MO denoting methyl oleate), and the fit indicates that 36% of the measured loss of OL is attributed to secondary chemistry. See Sect. 4.4.3.1 and Hearn et al. (2005) for details (from Hearn et al., 2005).

11173

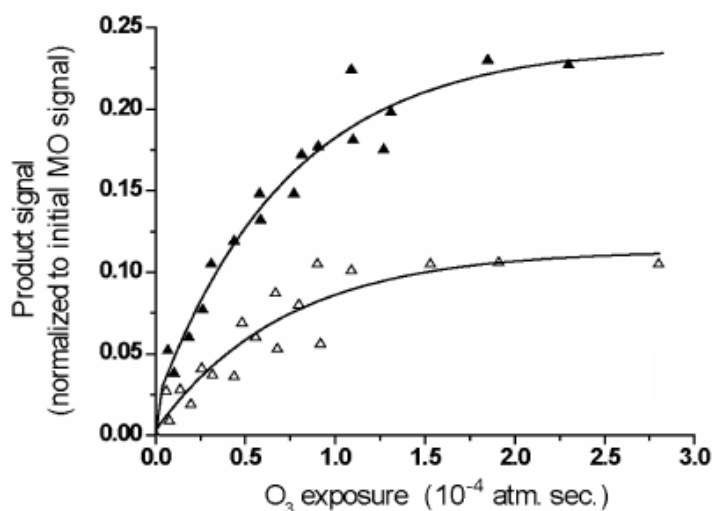


Fig. 8. Appearance of Cl rearrangement products (9-methoxy-9-oxononanoic acid) with progressive ozone exposure. The yield is lower in mixed OL/MOL particles (Δ) (methyl oleate is denoted MO on this figure) than pure MOL particles (▲), indicating a sizable reaction between Cl and OL. Lines are to guide the eye and do not represent fits to the data (from Hearn et al., 2005).

11174

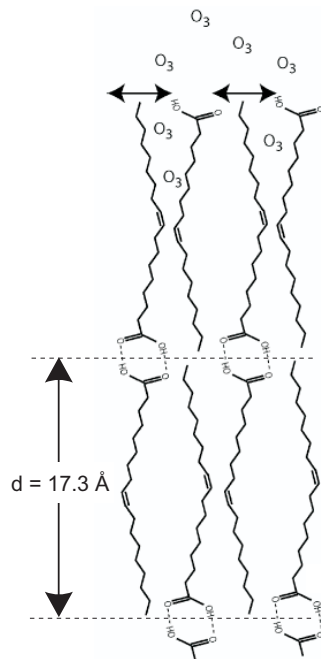


Fig. 9. Quasi-smectic condensed phase structure of OL dimers stabilized by hydrogen bonding. As suggested by Hearn et al. (2005), the alkyl chains will be more mobile than the rigid double bonds and form an O₃ “funnel” directing the O₃ towards the double bonds while inhibiting diffusion past them. This has been proposed to be the basis of the surface reactivity of this system evidenced by Hearn et al. (2005). The spacing indicated on the figure has been determined by Iwahashi et al. (1991) (adapted from Hearn et al., 2005).

11175

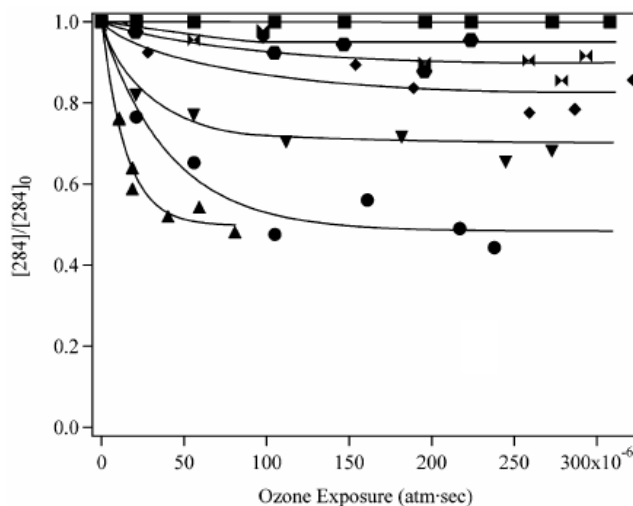


Fig. 10. Decay of SA from increasing O₃ exposure for OL/SA mixed particles as determined by Aerodyne AMS. (SA is denoted [284] in the figure). Key (OL/SA): 90/10 (▲), 75/25 (●), 60/40 (▼), 50/50 (○), 30/70 (◆), 10/90 (◆), 0/100 (■). Lines are to guide the eye and do not represent a fit to the data (from Katrib et al., 2005a).

11176

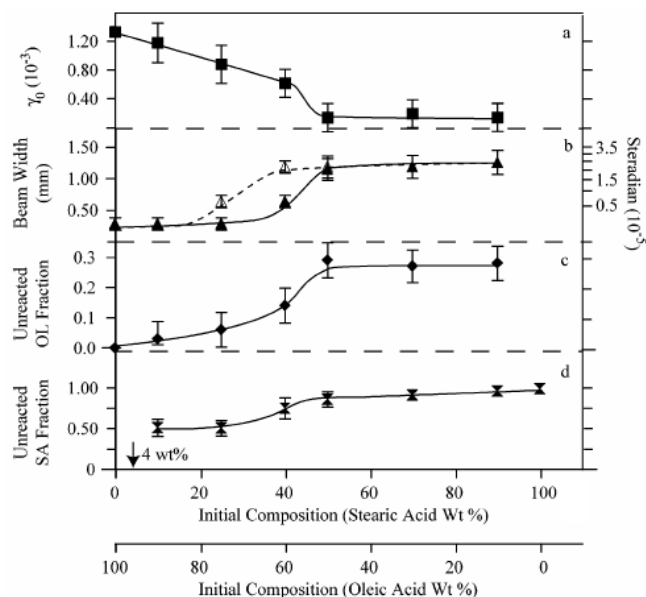


Fig. 11. Summary of results for increasing SA composition in OL/SA mixed particles: **(a)** initial reactive uptake coefficient (γ_o); **(b)** beam width before (\blacktriangle) and after (\triangle) ozone exposure (300×10^{-6} atm s O_3); **(c)** unreacted OL fraction after ozone exposure; **(d)** unreacted SA fraction after ozone exposure. Quantities are shown for increasing SA weight percent composition, with the balance being OL. Lines are to guide the eye and do not represent a model fit. The amount 4 wt% indicates the composition of a liquid with pure, solid SA at 298 K (Inoue et al., 2004). For more details please refer to Sect. 4.4.3.2 in this report or the original work by Katrib et al. (2005a) (from Katrib et al., 2005a).

11177

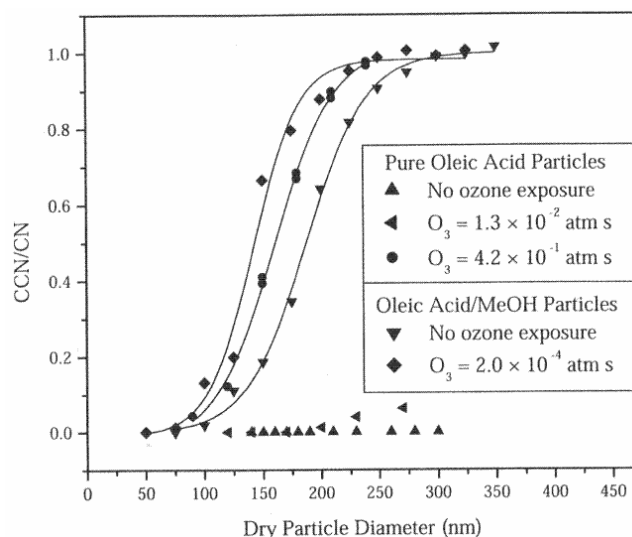


Fig. 12. CCN/Condensation nuclei (CN) ratio as a function of initial dry particle diameter at a supersaturation of 0.6% for several ozone exposures. All dry diameters represent the diameter after oxidation. Results for both pure OL and OL/methanol mixed particles are shown (from Broekhuizen et al., 2004).

11178

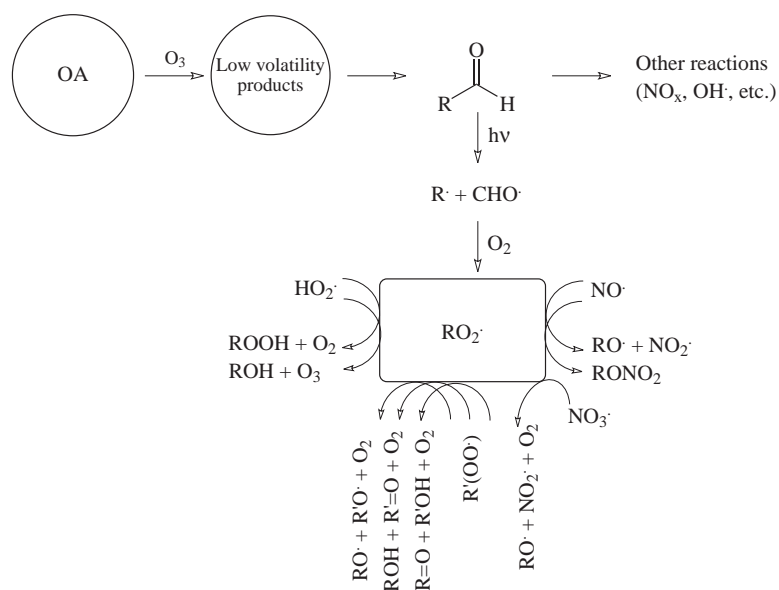


Fig. 13. Photolysis of aldehydes in the troposphere with emphasis on the chemical fate of the alkyl radical. As discussed in 5.4, the conversion of the alkyl radical ($\text{R}\cdot$) to the organic peroxy radical ($\text{RO}_2\cdot$) is the prevalent fate of the former species in the troposphere. Depicted are a variety of reactions that the organic peroxy radical can undergo in the troposphere demonstrating how emitted aldehydes can increase the oxidative capacity of that stratum.